Accepted Manuscript

Synthesis and biological evaluation of new aryl-alkyl(alkenyl)-4-benzylpiperidines, novel Sigma Receptor (SR) modulators, as potential anticancer-agent

Marta Rui, Daniela Rossi, Annamaria Marra, Mayra Paolillo, Sergio Schinelli, Daniela Curti, Anna Tesei, Michela Cortesi, Alice Zamagni, Erik Laurini, Sabrina Pricl, Dirk Schepmann, Bernhard Wűnsch, Ernst Urban, Vittorio Pace, Simona Collina

PII: S0223-5234(16)30725-5

DOI: 10.1016/j.ejmech.2016.08.067

Reference: EJMECH 8863

To appear in: *European Journal of Medicinal Chemistry*

Received Date: 20 July 2016

Revised Date: 29 August 2016

Accepted Date: 30 August 2016

Please cite this article as: M. Rui, D. Rossi, A. Marra, M. Paolillo, S. Schinelli, D. Curti, A. Tesei, M. Cortesi, A. Zamagni, E. Laurini, S. Pricl, D. Schepmann, B. Wűnsch, E. Urban, V. Pace, S. Collina, Synthesis and biological evaluation of new aryl-alkyl(alkenyl)-4-benzylpiperidines, novel Sigma Receptor (SR) modulators, as potential anticancer-agent, *European Journal of Medicinal Chemistry* (2016), doi: 10.1016/j.ejmech.2016.08.067.

Synthesis and biological evaluation of new aryl-alkyl(alkenyl)-4-benzylpiperidines, novel Sigma Receptor (SR) modulators, as potential anticancer-agent.

Marta Rui[1,3#], Daniela Rossi[1#], Annamaria Marra[1], Mayra Paolillo[2], Sergio Schinelli[2], Daniela Curti[4], Anna Tesei[5], Michela Cortesi[5], Alice Zamagni[5], Erik Laurini[6], Sabrina Pricl[6,7], Dirk Schepmann[8], Bernhard Wűnsch[8], Ernst Urban[3], Vittorio Pace[3], Simona Collina[1*]

[1]*Department of Drug Sciences, Medicinal Chemistry and Pharmaceutical Technology section, University of Pavia, Viale Taramelli 6 and 12, 27100 Pavia (Italy)*

[2]*Department of Drug Sciences, Pharmacology section, University of Pavia, Viale Taramelli 6 and 12, 27100 Pavia (Italy)*

[3]*Department of Pharmaceutical Chemistry, University of Vienna, Althanstrasse 14, 1090 Vienna (Austria)*

[4]*Department of Biology and Biotechnology "L. Spallanzani", Lab. of Cellular and Molecular Neuropharmacology, University of Pavia, Via Ferrata 9, 27100 Pavia (Italy)*

[5]*Radiobiology and Preclinical Pharmacology Laboratory, Biosciences Laboratory, Istituto Scientifico Romagnolo per lo Studio e la Cura dei Tumori (IRST) IRCCS, Via P. Maroncelli 40, 47014 Meldola (FC), Italy*

[6] *MOSE – DEA, University of Trieste, Piazzale Europa 1, 34127 Trieste (Italy)*

[7]*National Interuniversity Consortium for Material Science and Technology (INSTM), Research Unit MOSE-DEA University of Trieste, Trieste, Italy*

[8]*Institute of Pharmaceutical and Medicinal Chemistry, University of Muenster, Correnstrasse 48, 48149 Muenster (Germany)*

[*]Correspondence to: Simona Collina, Department of Drug Sciences, Medicinal Chemistry and Pharmaceutical Technology section, University of Pavia, Viale Taramelli 12, 27100 Pavia (Italy). Phone: (+39)0382-987379, Fax: (+39)0382-422975. E-mail: simona.collina@unipv.it

[#]These Authors equally contributed to this work

Abstract

In the early 2000s, the Sigma Receptor (SR) family was identified as potential "druggable" target in cancer treatment. Indeed, high density of SRs was found in breast, lung, and prostate cancer cells, supporting the idea that SRs could play a role in tumor growth and progression. Moreover, a link between the degree of SR expression and tumor aggressiveness has been postulated, justified by the presence of SRs in high metastatic-potential cancer cells. As a consequence, considerable efforts have been devoted to the development of small molecules endowed with good affinity towards the two SR subtypes (S1R and S2R) with potential anticancer activity. Herein we report the synthesis and biological profile of aryl-alkyl(alkenyl)-4-benzylpiperidine derivatives - as novel potential anticancer drugs targeting SR. Among them, **3** (RC-106) exhibited a preclinical profile of antitumor efficacy on a panel of cell lines representative of different cancer types (*i.e.* Paca3, MDA-MB 231) expressing both SRs, and emerged as a *hit* compound of a new class of SRs modulators potentially useful for the treatment of cancer disease.

Keywords
Sigma Receptor (SR); pan-SR modulators; compound 3 (RC-106); S1R agonist/antagonist profile; potential anticancer property; apoptotic pathway.

1. Introduction

Sigma receptors (SRs) are an enigmatic receptor family localized in plasmatic, mitochondrial and endoplasmic reticulum membranes of several organs including liver, kidney and brain. Radioligand binding studies and biochemical analyses have shown the presence of two SR subtypes, Sigma 1 (S1R) and Sigma 2 (S2R) receptors with different anatomical distribution, distinct physiological and pharmacological profiles [1-4].

It is well known that S1Rs play critical roles in the mammalian nervous system, indeed their involvement in different neurodegenerative and neuropsychiatric diseases has been well documented [5-8]. Their ligands can yield both cytoprotective or cytotoxic actions. In detail, S1R agonists promote neuroprotection, neurite outgrowth, trophic factor production as well as microglial activation, mitochondrial integrity and reduce production

of reactive oxygen species [9,10]. As a consequence, S1R agonists display a high therapeutic potential for Central Nervous System (CNS) pathologies such as Amyotrophic Lateral Sclerosis, Multiple Sclerosis, Alzheimer's disease and Parkinson disease [5,11,12]. Conversely, S1R antagonists may play a role in neuropathic pain and anticancer therapy. Overexpression of S1R in high metastatic potential cancer cells, together with the efficacy of the S1R antagonist Rimcazole (Fig. 1) in inhibiting tumor cell survival and in promoting apoptosis in breast cancer cells (MCF-7, MDA-MB-231, MDA-MB-157 and T47D) suggests a link between the degree of S1R expression and tumor growth and aggressiveness [13]. Despite the evidence supporting the importance of S1R in cancer, the mechanism of action of S1R antagonists in causing cell death is still unclear. Currently, it has been hypothesized that the observed apoptototic phenomena are related to the increase of intracellular calcium levels [14-16].

The S2R subtype is still largely unknown: it has not been cloned yet and its molecular structure has not been clarified . In the intracellular environment, S2R binding sites are localized in mitochondria, lysomes, endoplasmic reticulum, and plasma membrane. Recent studies describe how S2R ligands trigger a cell response which inhibit the activity of the P-glycoprotein, responsible for the active extrusion of anticancer drugs, leading to cell death. [17,18]. Moreover, the hypothesis of a correlation between S2R and Progesterone Receptor Membrane Component 1 (PGRMC1) [19,20] supports the idea that S2R may exert a critical role in tumorigenesis [18]. Indeed, the over-expression of PGRMC1 has been associated to tumor stage and to actively proliferating and invasive cancer cells [21]. It is also relevant that proliferating breast carcinoma cells express S2R up to ten times more than quiescent cells, and the degree of S2R expression has been correlated with tumor staging and grading [22-24]. The highest level of S2R has been detected in pancreatic cancer cell lines (Panc-02, Panc-01, CFPAC-1, AsPC-1) [25]. A recent study, carried out on mouse breast cancer (EMT-6) and human melanoma (MDA-MB-435) cell lines, demonstrate that siramesine (Fig. 1), a S2R selective ligand commonly used as reference compound, can induce cell death (with an EC_{50} in both cell lines lower than 10 μM) by three different mechanisms: caspase activation, autophagy, and impaired cell-cycle progression [26]. In the same work, it has been also demonstrated that other S2R ligands, *i.e.* SV119, WC-26 and RHM-138 (Fig. 1), possess a cytotoxic

effect in the micromolar range in the aforementioned cancer cell lines [26]. Moreover, the same compounds are able to inhibit proliferation of pancreatic cancer cells (human lines: BxPC3, AsPC1, Cfpac, Panc1 and PaCa-2; murine line: Panc02) with an $IC_{50} \leq 100$ µM [25].

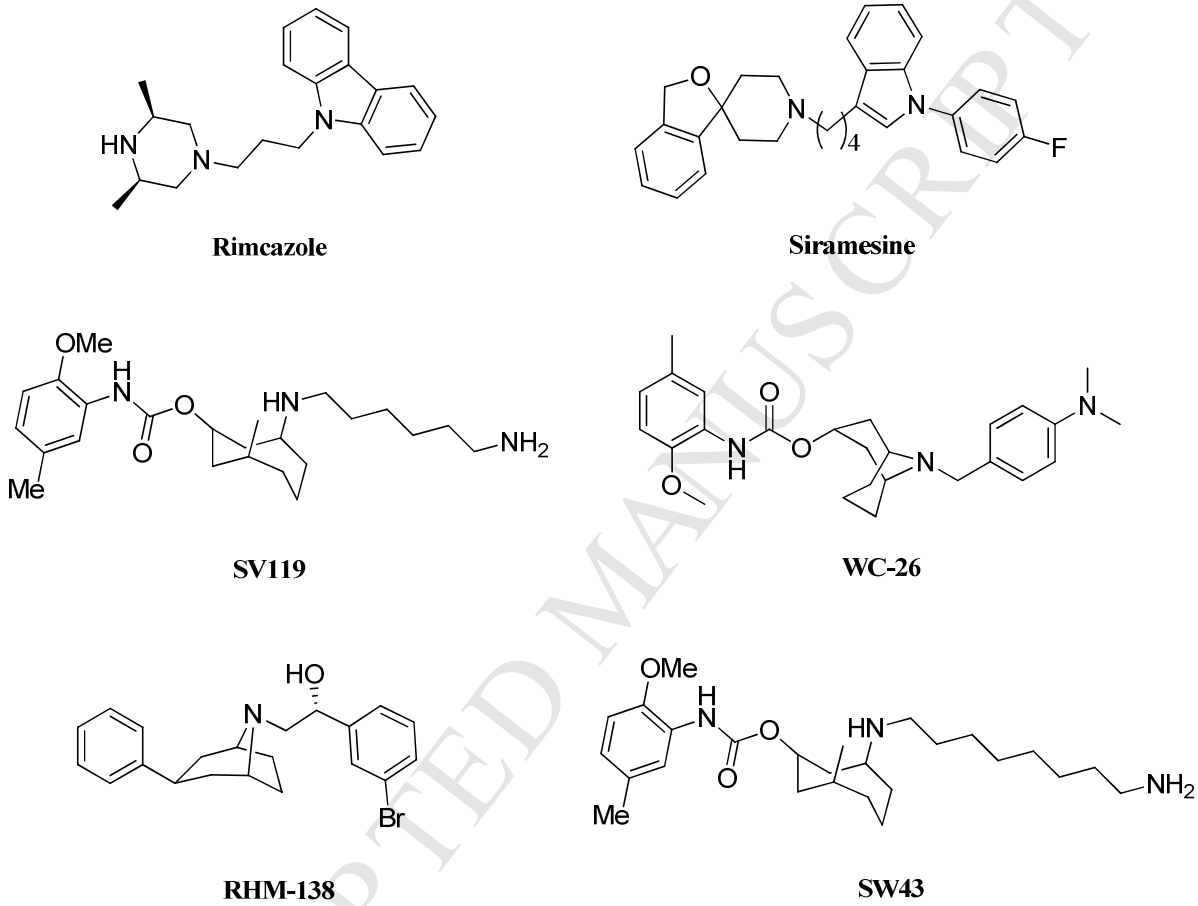

Fig. 1. S1R and S2R compounds able to promote antiproliferative effects. Rimcazole (KiS1 = 908.0 ± 99 nM; KiS2 = 302.0 ± 37 nM) [27]. **Siramesine** (KiS1 = 17.0 nM; KiS2 = 0.12 nM); **SV119** (KiS1 = 1417.0 nM; KiS2 = 5.2 nM); **WC-26** (KiS1 = 1436.5 ± 166.1 nM; KiS2 = 2.58 ± 0.59 nM); **RHM-138** (KiS1 = 544.0 nM; KiS2 = 12.3 nM); **SW43** (KiS1 = 133.0 nM; KiS2 = 19.0 nM) [28].

On the bases of the above findings, we reasoned that both S1R antagonist and S2R agonists could be useful tools to address novel and more focused cancer treatments. Hence, SRs could represent an exciting target to develop anticancer drugs with novel mechanisms of action. Our group has previously prepared and characterized a wide series of compounds with preferential affinity towards S1R [29a-d]. In an intriguing

observation, we documented that the presence of the bulky 4-benzylpiperidine moiety, while preserving high binding strength for S1R, increases the affinity towards S2R [29c]. Therefore, in the present study we present our efforts aimed at the identification and characterization of potent SR modulators, able to bind both receptor subtypes. Specifically, we report herein the preliminary structure-activity relationship (SAR) (Fig. 2) of aryl-alkyl(alkenyl)-4-benzylpiperidines with the general structure of Fig. 2. Derivatives **3** and **6** that displayed good affinity toward both receptor subtypes, from now on called pan-SR ligands, were passed for testing *in vitro* cytotoxic activity evaluation. To validate the hypothesis that S1R and S2R modulators could be effective as anticancer drugs, compound **3** was next screened towards a panel of tumor cell lines representative of various cancer types, all expressing both sigma receptors. The results of our studies showed that **3**, called by us RC-106, has interesting anticancer activities against prostate, glioblastoma, pancreas and breast cancer cell lines. The activity against pancreatic PaCa3 cells is of particular interest, being **3** (RC-106) effective against actively proliferating cells (IC_{50} = 42 μM) and against cells with reduced proliferation rate (IC_{50} = 7.0 μM,). The results of this effort are described below.

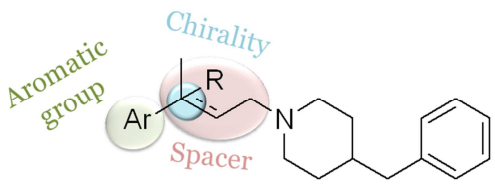

Fig. 2. SAR exploration. Structural elements subjected to variation are highlighted.

2. Results

2.1. Chemistry

The preparation of compounds **1-12** is summarized in Scheme 1. In cases where a chiral center was present, (semi)preparative chiral chromatography was used to isolate the stereoisomers.

The key intermediate of the synthetic process is the β-aminoketone **A**. The synthetic pathway to obtain **A** was already described by us and involves a Michael addition of 4-benzylpiperidine to but-3-en-2-one in absolute ethanol and glacial acetic acid, followed

by purification *via* acid/basic extraction, as reported in our previous work [29c]. The subsequent lithiation reaction at aryl-bromine in anhydrous Et_2O at -78 °C with *t*-butyl lithium, followed by addition/substitution reaction in the presence of the β-aminoketone **A** and quenching with H_2O, led to isolate crude compounds. After purification *via* acid/basic extraction, **1** and **2** in sufficient amount for the subsequent reaction an suitable purity for biological assay were obtained, as confirmed by ^{1}H-NMR, ^{13}C-NMR and UPLC-MS analysis.

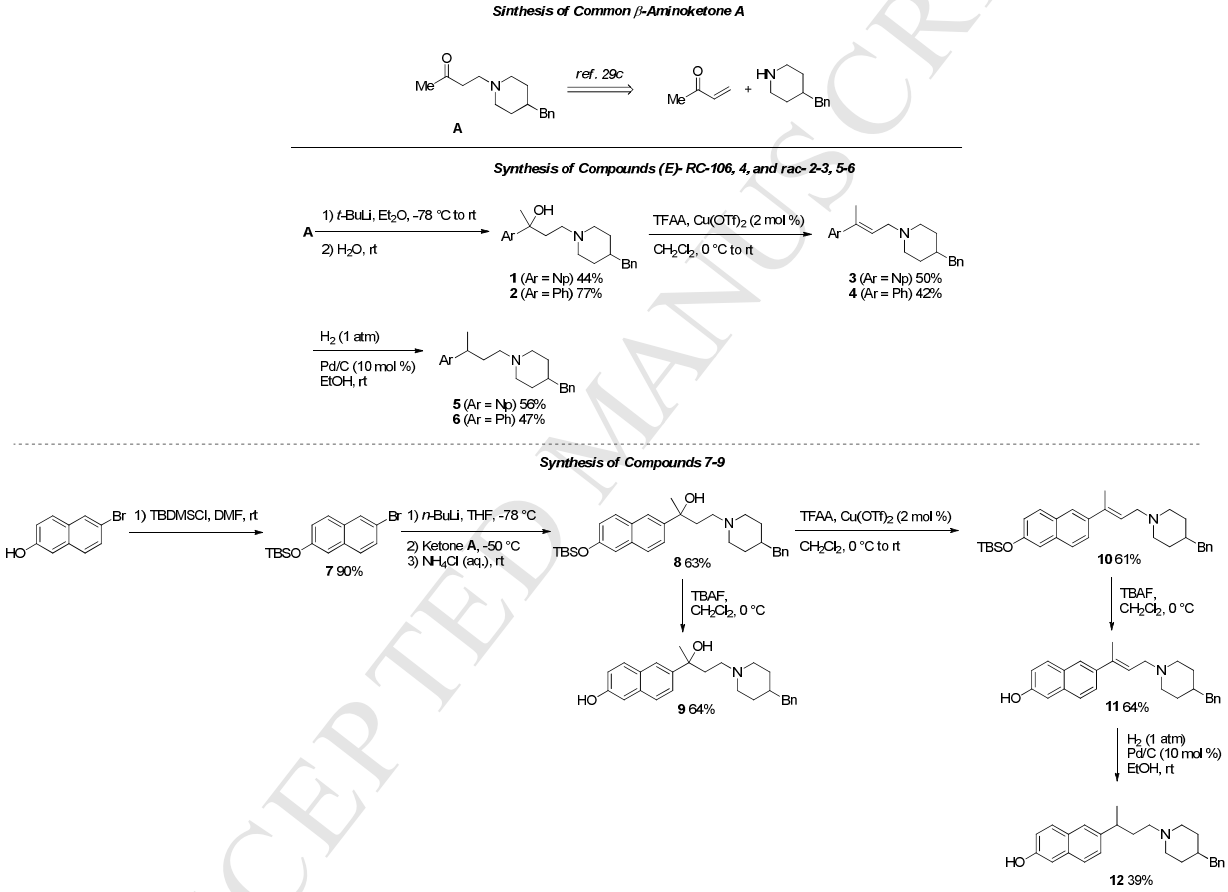

Scheme 1. Synthesis of compounds 1-12.

Arylalkylaminoalcohols **1** and **2** were treated with trifluoroacetic anhydride in the presence of a catalytic amount of cupper triflate, according with a procedure already experimented by us [30]. In this way, compounds **3** and **4**, as (*E*) stereoisomers C2-C3, together with low amounts of the olefinic regioisomers C3-C4, were obtained as evidenced by ^{1}H-NMR. It is worth noting that no signals related to the (*Z*) stereoisomer, which represented the minor product using the standard acidic conditions (37% HCl)

[29b] were present in the ^{1}H-NMR of crude products. As a further step, an amount of arylalkenylamines were subjected to catalytic reduction reaction in hydrogen atmosphere in the presence of Pd (0)/C 10% (p/p) in absolute EtOH, giving rise to the corresponding arylalkylamines **5** and **6**. Crude **3-6** were purified using alumina (II Brockmann degree) column chromatography, yielding pure compounds as confirmed by ^{1}H-NMR, ^{13}C-NMR and UPLC-MS analysis.

In the case of compounds bearing the hydroxyl group at the naphtylic moiety, an additional step was required, consisting in the protective reaction of the –OH group by *t*-butyldimethylsilyl chloride, thus obtaining **7** which was lithiated in anhydrous THF at -78 °C using an excess of *n*-butyl lithium. After 20 minutes, the aminoketone **A** was added to the C-lithiated intermediate, keeping the temperature below -50 °C for 1.5 h. The reaction was quenched with saturated aqueous NH_4Cl and extracted with Et_2O. The crude product was purified by column chromatography giving **8**. An amount of this compound was subjected to an elimination reaction using trifluoroacetic anhydride in the presence of a catalytic amount of cupper triflate to give the arylalkenylamine **10** [(*E*) stereoisomer C2-C3] as main compound, easily isolated by column chromatography. Compounds **8** and **10** were then subjected to the deprotection of –OH-aromatic by drop wise addition of tetra-N-butylammonium fluoride at 0 °C in argon atmosphere in anhydrous dichloromethane (DCM), to give **9** and **11**, respectively. Lastly, the reduction reaction of **11** using a catalytic amount of Pd (0) in hydrogen atmosphere gave rise to arylalkylamine **12**. With the exception of compound **11**, which was purified by treatment with methanol, pure **9** and **12** were obtained after purification through silica column chromatography. Also in the case of naphthol-derivatives **9** and **11-12**, the identities were confirmed by ^{1}H-NMR, ^{13}C-NMR and UPLC-MS analysis.

All potential SR modulators **1-6**, **9** and **11-12** were obtained in a sufficient amount and with the appropriate degree of purity for the subsequent biological investigations and, in the case of racemic compound, also for HPLC chiral resolution.

2.2. Chiral resolution

To investigate the relationship between stereochemistry and receptor binding affinity, we prepared enantiomeric **1-2**, **5-6**, **9** and **12**. On the bases of our previous experience, a direct chiral HPLC method of enantiomeric separation was applied, and the scaling up of the process was performed [31a-e]. Baseline separation of racemates was obtained using cellulose and amylose derived chiral stationary phases (Chiralcel OJ-H, Chiralpack IC and Chiralpack IA), under different elution conditions, including different mixtures of *n*-heptane and polar modifiers (methanol, ethanol or 2-propanol) and alcohols (methanol, ethanol and 2-propanol). In all cases 0.1 % of diethylamine (DEA) was added to the mobile phase. Moreover, in the case of the Chiralpak IC, the analysis were carried out also in the presence of 0.3 % of trifluoroacetic acid (TFA), which improves enantiomer separations. The optimized analytical methods (Table 1, Fig. SI1, see Supplementary material) were suitably transferred to the (semi)preparative scale. In detail, enantiomeric **1**, **2**, **5** and **9** were resolved by a (semi)preparative Chiralcel OJ-H column, eluting with ethanol and 0.1 % diethylamine (for the compound **1**) or methanol and 0.1 % diethylamine (for the compounds **2**, **5** and **9**), whereas compounds **6** and **12** were resolved on (semi)preparative Chiralpak IA, using methanol and 0.1 % of diethylamine, in all cases eluting at a flow rate of 2.5 mL/min. The elution conditions applied provided a quick access to the desired enantiomers (Table 2) with enantiomeric excess over than 95%, as evidenced by analytical control of the collected fractions , and in sufficient amount for preliminary biological assays.

Table 1. Analytical chiral resolution of **1-2**, **5-6**, **9** and **12**.

Compound	Column	Eluent	K_1	K_2	α	Rs
1	Chiralcel OJ-H	A	1.03	1.63	1.58	3.25
2	Chiralcel OJ-H	B	1.24	1.80	1.45	4.05
5	Chiralcel OJ-H	B	3.98	4.80	1.21	2.46
6	Chiralpak IA	B	0.57	0.81	1.42	3.06
9	Chiralcel OJ-H	B	1.10	1.61	1.46	2.62
12	Chiralpak IA	B	0.96	1.27	1.32	2.49

Eluent: A (100% ethanol, 0.1 % diethylamine); B (methanol 100%, 0.1 % diethylamine), flow rate: 1 mL/min; detection UV at 220 (compounds **2** and **6**) and at 254 nm (compounds **1**, **5**, **9** and **12**).

Table 2. Chiroptical properties of enantiomeric **1-2**, **5-6**, **9** and **12**.

Compound	$[\alpha]_D^{20}$ (c% in MeOH)	ee (%)[a]	*K*
1a	+ 40.5 (0.2)	96.0	1.03
1b	- 42.3 (0.2)	97.0	1.63
2a	+ 10.5 (0.6)	99.9	1.24
2b	- 9.2 (0.6)	98.0	1.80
5a	+ 6.1 (0.2)	95.0	3.98
5b	- 6.3 (0.2)	95.0	4.80
6a	+ 8.2 (0.3)	99.9	0.57
6b	- 8.3 (0.3)	99.9	0.81
9a	+ 24.2 (0.1)	99.9	1.10
9b	- 24.8 (0.1)	99.9	1.61
12°	+ 11.8 (0.3)	99.9	0.96
12b	- 12.0 (0.3)	99.9	1.27

[a] Determined by chiral HPLC under the analytical conditions reported in Table 1.

2.3. SAR studies

The S1R and S2R binding site affinities of the tested compounds were determined in competition experiments using radioligands. All compounds were tested on guinea pig brain and rat liver membranes obtained by homogenization, centrifugation, and washing of the respective tissues. ~~Both~~ S1R ~~and S2R~~ binding site assays were performed with [^{3}H]-(+)-pentazocine as radioligand. The S2R binding values were evaluated using [^{3}H]-DTG ~~was used~~ as radioligand ~~in the S2R assays~~. Compounds with high affinity were tested three times. For compounds with low SR affinity, only one measure was performed. The SR affinities of all compounds towards both S1R and S2R are presented in Table 3.

Table 3. Binding affinities towards S1R and S2R. Values are expressed as mean ± SEM of three experiments.

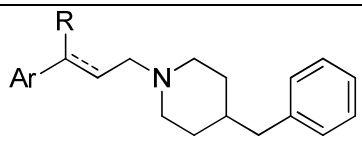

Compound	Ar	R	K_iS1 ± SEM	K_iS2 ± SEM
1	2-naphtyl	OH	6.9 ± 2	62.5
1a	2-naphtyl	OH	10 ± 2	81 ± 35
1b	2-naphtyl	OH	11 ± 1	79 ± 21
2	Phenyl	OH	9.8 ± 4	57 ± 11
2a	Phenyl	OH	27 ± 9	339[a]
2b	Phenyl	OH	40 ± 4	240[a]
3	2-naphtyl	-	12 ± 5	22 ± 3
4	Phenyl	-	0.7 ± 1	47± 13
5	2-naphtyl	H	5.6 ± 3	144[a]
5a	2-naphtyl	H	6.0 ± 0.5	26± 9
5b	2-naphtyl	H	6.9 ± 1	98
6	Phenyl	H	2.1 ± 1	6.5 ± 3
6a	Phenyl	H	2.9 ± 0.4	8.9 ± 2.1
6b	Phenyl	H	3.0 ± 0.3	7.9 ± 1.9
9	6-hydroxy naphtyl	OH	27 ± 5	118[a]
9a	6-hydroxy naphtyl	OH	70 ± 21	68 ± 8
9b	6-hydroxy naphtyl	OH	62 ± 4	905[a]
11	6-hydroxy naphtyl	-	9.6 ± 3	305[a]
12	6-hydroxy naphtyl	H	59 ± 5	314[a]
12a	6-hydroxy naphtyl	H	35± 2	582[a]
12b	6-hydroxy naphtyl	H	13 ± 4	105[a]

[a] Compounds with high affinity were tested three times. For compounds with low SR affinity (> 100 nM), only one measure was performed.

All compounds, with the only exception of **9a**, **9b** and **12**, showed an interesting affinity towards S1R (K_iS1 ≤ 50 nM) and a good/modest affinity towards S2R, with the exception of compounds **2a**, **2b**, **9** and **12**, which are weak S2R binders. Particularly, all the arylalkylaminoalcohols **1**, **2** and **9** showed a preference affinity towards S1R and the first

eluted enantiomers exhibit a slight preferential interaction with the target, in accordance with our previous work [32]. Conversely, SRs do not show stereoselectivity towards the enantiomer of arylalkylamines, confirming our previous findings [31a-b]. Of particular interest are compounds **3** and **6** (racemic and enantiomeric), having a good affinity towards both S1R and S2R.

To propose a molecular rationale for the experimental affinity of the new 4-benzylpiperidine derivatives for the S1R, we used our validated three-dimensional model of the S1R [29d,31a-b,33-35]. We applied a consolidated simulation recipe based on free energy of binding (ΔG_{bind}) estimation in the framework of the Molecular Mechanics/PoissonBoltzmann Surface Area (MM/PBSA) computational methodology (Tables SI1, see Supplementary material) [36]. Taking the naphthalene derivative **3** as a proof-of-concept, the analysis of the corresponding MD trajectory reveals that 4-benzyl-piperidine moiety establishes a strong network of polar and hydrophobic interactions with the receptor. As shown in Fig. 3A and B, the piperidine nitrogen atom is engaged in the prototypical salt bridge with the carboxylic side chain of Asp126, while the aliphatic portion of the heterocycle together with the benzyl ring are perfectly encased in the hydrophobic S1R cavity lined by residues Ile128, Phe133, Tyr173 and Leu186. Finally, the naphthalene group of **3** performs stabilizing π interactions with the side chains of Arg119 and Trp121.

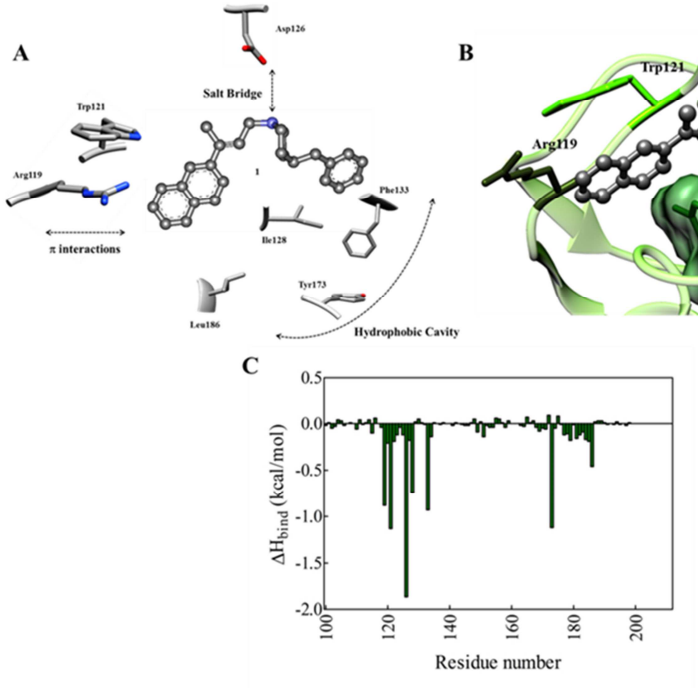

Fig. 3. (A) 2D schematic representation of the identified interactions between the S1R 3D model and **3**. (B) Zoomed view of SR1 in complex with **3**. The compound is in atom colored sticks-and-balls (C, gray; N, blue). Hydrogen atoms, water molecules, ions, and counterions are not shown for clarity. A dashed black line highlights the salt bridge between the S1R D126 side chain and the piperidine nitrogen atom of **3**. (C) Per-residue binding enthalpy ($\Delta H_{bind,res}$) decomposition for the S1R/**3** complex. Only SR1 amino acids from positions 100 to 200 – most relevant to ligand binding - are shown for clarity.

For each compound, a quantitative analysis of ligand/protein interactions was next performed *via* a per-residue deconvolution of the enthalpic contribution to binding (Fig. SI3, see Supplementary material). Taking again compound **3** as reference, Fig. 3C shows the resulting interaction spectrum. Substantially, the hydrophobic interactions of **3** with the side chains of residues Ile128, Phe133, Tyr173, and Leu186 contribute an overall stabilization term to binding equal to -3.25 kcal/mol, while the permanent salt bridge between the N-atom of **3** and the side chain of Asp126 (average dynamic length (ADL) = 4.09 ± 0.04 Å) reflects in a stabilizing contribution of -1.87 kcal/mol. Finally, the important π/π and π/cation interactions (established between the naphthyl ring of the molecule and the indole ring of Trp121 and the cationic side chain of Arg119, respectively) result in a strong enthalpic stabilization of -2.01kcal/mol.

To sum up, compounds **3** and both racemic and enantiomeric **6** revealed good affinity towards S1R, in agreement with the molecular modelling studies, together with a S2R affinity and therefore they have been selected for a deeper biological investigation.

2.4. Quantification of SRs expression in cancer cell lines

As stated in the introduction section, an appropriate modulation of both receptors could have a synergic effect in inducing tumor cell death. Therefore, the first step of our in depth biological investigation consisted in testing a panel of cancer cell lines representative of different human solid tumors (Table 4) for SRs expression [37-40]. In details, we determined the expression levels of mRNA of S1R and PGRMC1, considered as the S2R binding site, by Real Time RT- Polymerase Chain Reaction (RT-PCR).

Table 4. Tumor cell lines expressing both SR selected for this study

Cell line	Origin	Tumor source	Morphology
Capan-2	Pancreas	Primary tumor	Epithelial
Paca3	Pancreas	Primary tumor	Epithelial
CFPaC-1	Pancreas	Metastatic site	Epithelial
SUM 159	Breast	Primary tumor	Epithelial
MDA-MB 231	Breast	Metastatic site	Epithelial
PC3	Prostate	Metastatic site	Epithelial
LNCaP	Prostate	Metastatic site	Epithelial
U87	Glioblastoma	Primary tumor	Epithelial

The expression values of S1R and PGRMC-1 in CFPAC-1 line are very similar as evidenced by western blot and related densitometric analysis showed in supplematary data (Fig. SI4) and for this reason were used as reference values (arbitrary set equal to 1) for Real Time RT-PCR evaluation of S1R or PGRMC-1 expression in the panel of cell line investigated. As shown in Fig. 4 the highest S1R mRNA expression levels were found in MDA-MB 231, LNCaP and PaCa3 cell lines, whereas PGRMC1 mRNA was found to be highly expressed in PC3, CAPAN-2, and PaCa3 cell lines, respectively.

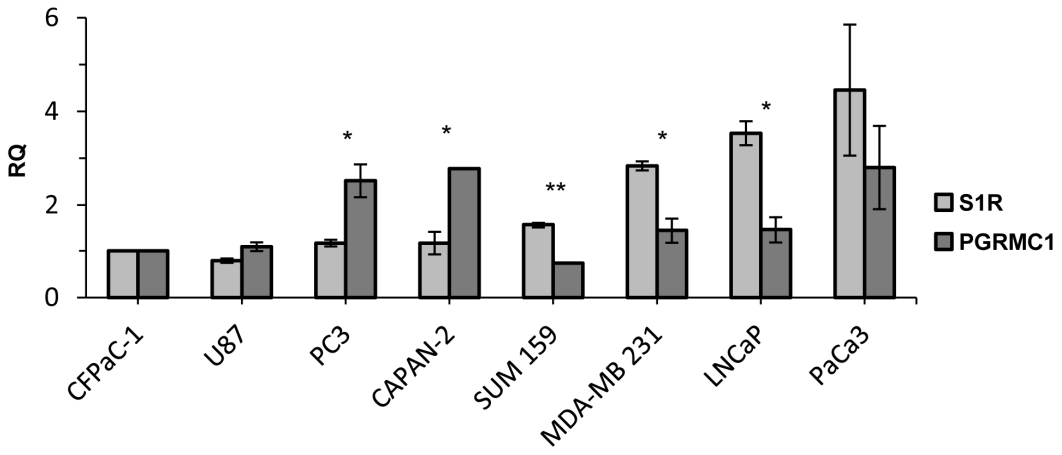

Fig. 4. Relative Quantification (RQ) of the target genes SR1 and PGRMC1 RNA expression. The mRNA levels were normalized to the endogenous reference genes GAPDH and HPRT, and quantified respect to the value of S1R or PGRMC-1 found in CFPaC-1 cell line that was arbitrary set equal to 1 (RQ=1). Values are the mean ± SD of three independent experiments.

*2.5. Preliminary biological evaluation of **3** and **6***

We perform a preliminary assessment of the anticancer potential of compounds **3** and **6**, showing a good affinity towards SRs, on PaCa3 cells that express both SRs at high level, using siramesine, a well known commercial S2R agonist, and NE100, a S1R antagonist, as reference compounds [26,41]. The effect of compounds **3**, **6**, siramesine and NE100 on cell viability was evaluated by the MTS assay. Cell lines grown in a 10% serum-containing medium were exposed to increasing concentrations of compounds (0.1 μM - 100 μM) for 24 hours. Compound **3** showed an interesting cytotoxic activity, comparable to siramesine, whereas compounds **6** and NE100 exhibited a poor cytotoxic effect (Fig. 5). Since fetal bovine serum (FBS) is enriched in a variety of growth factors and neurosteroids that may interfere and/or mask SR binding sites, the effect of compounds **3** and **6** on PaCa3 was evaluated also in serum-free medium. Interestingly, the decrease of cell viability induced by **3** was enhanced by starvation conditions (IC_{50} = 49.8 ± 4.1 μM and IC_{50} = 7.0 ± 0.2 μM, respectively). A similar effect was observed for siramesine (IC_{50} = 45.4 ± 2.0 μM in complete medium and IC_{50} = 6.0 ± 0.3 μM, in starvation condition). On the contrary, starvation conditions are irrelevant for the cytotoxic properties of **6** and NE100.

According to this data, compound **3**, by now on called RC-106, was selected for further investigation.

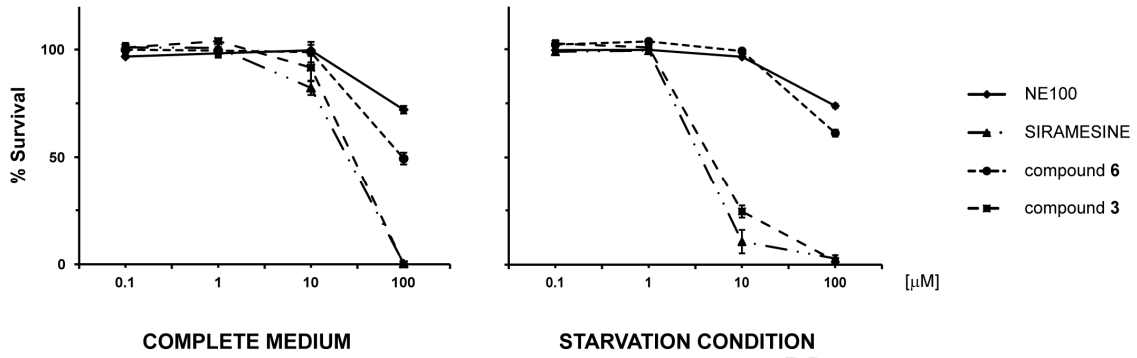

Fig. 5. Effect of different SR modulators. The cells were exposed to compounds NE100, Siramesine, **3** (RC-106) and **6**, for 24 hours in the presence or in the absence of 10% FBS. The viability of the cells was determined by MTS assay (mean ± SD of 3 independent experiments).

*2.6. S1R agonist/antagonist profile of compound **3** (RC-106)*

Considering that the anticancer activity of a S1R ligands is related to their antagonist profile [13], we investigated the profile of **3** (RC-106) by assessing its *in vitro* ability to modulate NGF-induced neurite outgrowth in PC12 cells. Indeed, S1R agonists are known to potentiate NGF-induced neurite outgrowth when used in the low micromolar concentration range [29c,31a]. In detail, PC12 cells were incubated in a medium containing 0.5% FBS plus NGF (2.5 ng/ml), in the presence of increasing concentrations of **3** (RC-106) (0-10μM) for 96 h. Subsequently, cells were fixed and those displaying a neurite longer than the diameter of the cell body were counted. Neurite outgrowth was not affected by the addition of **3** (RC-106) up to 1 μM concentration; on the other hand, starting from 2.5 μM neurite outgrowth was completely inhibited (Fig. SI3, see Supplementary material), thus suggesting a S1R antagonist profile. To confirm this hypothesis, competition assays were performed. Specifically, PC12 cells were incubated with the standard S1R agonist PRE-084 (5, 10 and 25μM) in the absence/presence of **3** (RC-106) at 0.25 or 2.5 μM. At 0.25 μM concentration, compound **3** (RC-106) significantly antagonized the effect of PRE-084 (10 and 25 μM) on NGF-induced neurite outgrowth (Fig. 6). At 2.5 μM concentration, **3** (RC-106) completely blocked NGF-

induced neurite sprouting, even in the presence of PRE-084 (results not shown). The results confirm that **3** (RC-106) is a S1R antagonist.

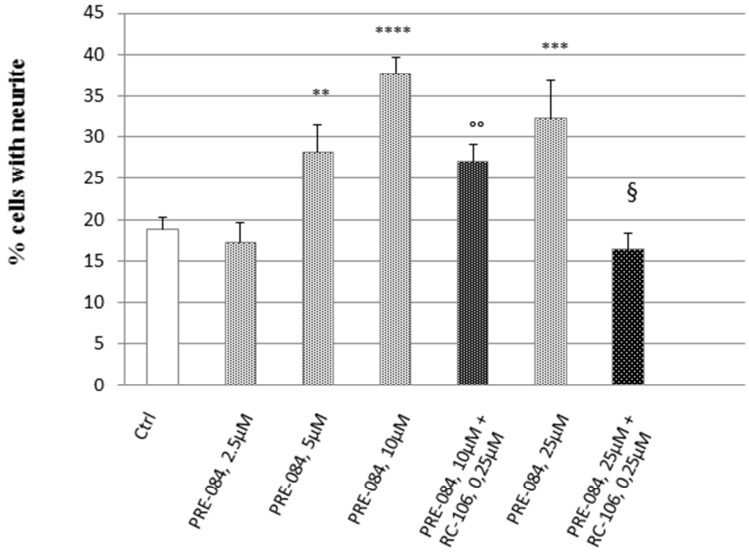

Fig. 6. Assay of NGF–induced neurite outgrowth in PC12 cells. Effect of PRE-084 alone or in combination with **3** (RC-106), at 0.25 µM. Histograms represent the mean±sem of at least 5 different experiments performed in triplicate. **= p<0.005; ***=p<0.0008; ****=p<0.000004 vs control (0 PRE-084). °°=p<0.007; °°°=p<0.00004 vs PRE-084 10µM and § = p<0.004 vs PRE-084 25µM.

*2.7. Effect of **3** (RC-106) on cell viability*

The cytotoxic acititvity of the pan-SR modulator **3** (RC-106) was evaluated by the MTS assay on the panel of cancer cell lines (LNCaP, PC3, U87, Paca3, Capan-2, MDA MB 231, SUM 159) expressing both S1R and S2R. Briefly, cell lines grown in a 10% serum-containing medium were exposed to increasing concentrations of **3** (RC-106) (0.1 µM - 100 µM) for 24 hours (Fig. 7). Compound **3** (RC-106) induced a decrease of cell viability in all cell lines starting at 25 µM, with IC_{50} values ranging from 50 µM to 64 µM. The IC_{50} values did not vary significantly by increasing the incubation time up to 48 h, except for the Paca3 cell line, whose IC_{50} value markedly decreased after 48 h incubation (28.73 ± 4.6, data not shown).

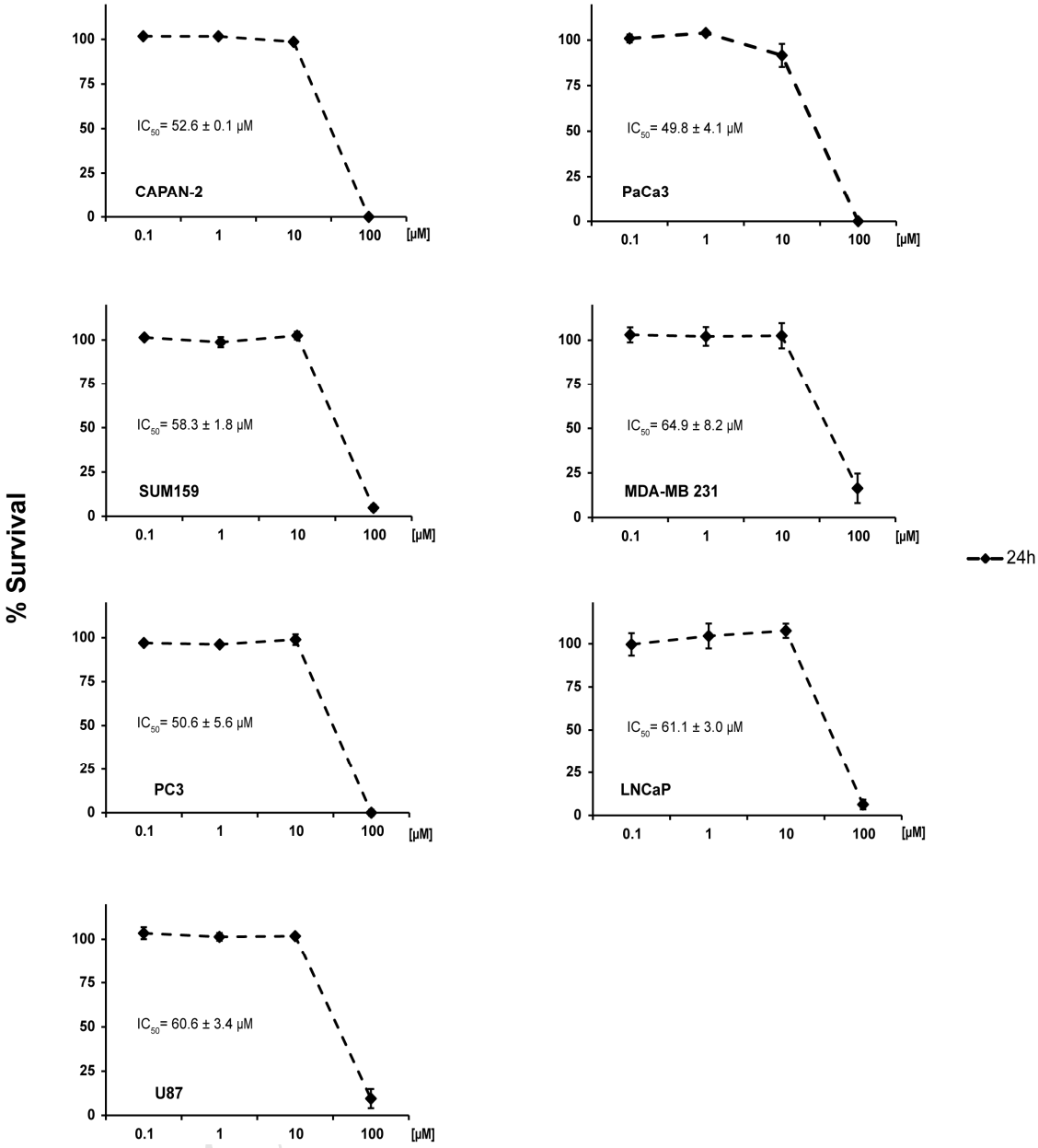

Fig. 7. Effect of 3 (RC-106) on cell viability was evaluated on a panel of cancer cell lines with different histotypes. Cells were exposed to the drug for 24 hours in a 10% FBS containing medium. Cell viability was determined by the MTS assay (average of three independent experiments ± SD).

The effect of **3** (RC-106) on U87, Capan-2 and LNCaP cancer cells in the absence of serum-induced cell cycle stimulation was also evaluated. Interestingly, in all the cell lines treated with **3** (RC-106) in serum-free conditions, a marked decrease of cell survival at low compound **3** (RC-106) concentrations compared to cells treated in FBS containing

medium, was shown, as evidenced by the low IC_{50} values (9.6 -10.5 µM) (Fig. 8). This trend is similar to that already evidenced on PaCa3 cells.

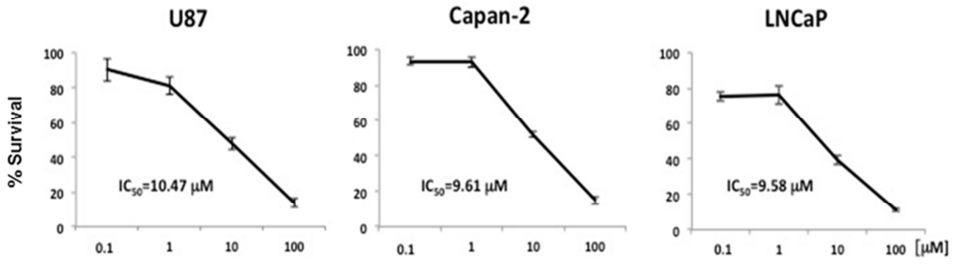

Fig. 8. **MTS assay in serum-free conditions.** After a 24 hours starvation, cell lines were treated for 24 hours with the indicated concentrations of **3** (RC-106). Data are expresses as percent of control values ± standard deviation.

*2.8. Study of **3** (RC-106) apoptotic pathway through capase 3 activation*

Lastly, to evaluate whether the observed decrease of cell viability under both conditions was due to apoptosis, TUNEL and Annexin V stainings (analyzed by FACS) and caspase 3 activation (western blot, WB) were performed on PaCa3 cells, the tumor line displaying also the highest PGRMC1 mRNA levels. Moreover, according to Zeng C. *et al.* [42] we adopted caspase 3 assay in order to clarify the S2R agonist/antagonist profile of **3** (RC-106).

The TUNEL assay showed that in serum containing medium a significant induction of apoptosis after 24 h exposure to **3** (RC-106) could be observed only at 25 µM concentration (Fig. 9A). This result is supported by the detection of the cleaved form of caspase 3 by WB analysis (Fig. 9C) and by the Annexin V assay. In these FACS experiments, a significant increase of early and late apoptotic cells (43.1% ± 3.4 and 34.1% ± 8.2, respectively) at 25 µM compound **3** (RC-106) was detected (Fig. 9B).

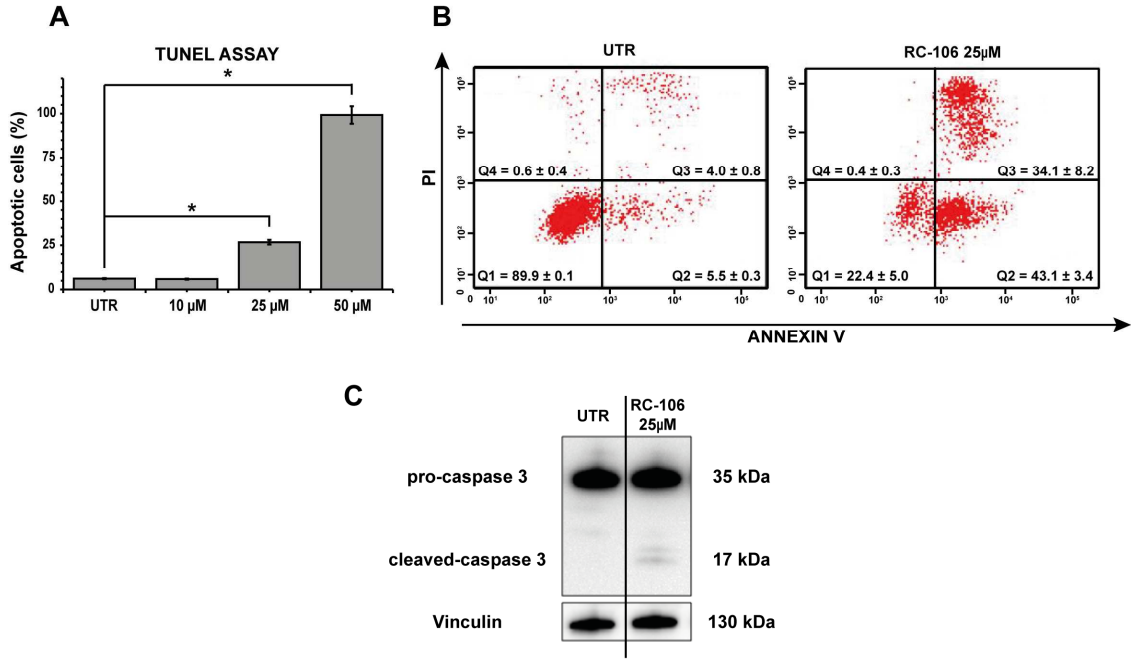

Fig. 9. Apoptosis and apoptotic-related markers analysis in Paca3 cells grown in 10% FBS complete medium. (A) TUNEL assay. Percentage of apoptotic cells after 24 h exposure to compound **3** (RC-106) at 10, 25 and 50 µM. *p<0.05. (B). Cytofluorimetric (FACS) analysis of apoptosis by Annexin V test. Cells were exposed for 24 h to compound **3** (RC-106) (25 µM). Q1 area represents viable cells; Q2 early-apoptotic cells; Q3 late-apoptotic cells; Q4 necrotic cells. The images are representative of three experiments. (C) WB analysis of apoptotic-related marker after 24 h exposure to **3** (RC-106) at 25 µM. Images are representative of two independent experiments.

When the same experiments were repeated under serum-free conditions (Fig. 10), a significant increase of apoptotic cells was detected by FACS analysis. In particular, at 10 µM, **3** (RC-106) induces significant apoptosis in PaCa3 cells (early apoptotic cells = 10.9 % ± 0.0 and late apoptotic cells = 17.2 % ± 0.6). The apoptosis induction was further confirmed by WB detection of cleaved caspase 3, after exposure of the cells at the same **3** (RC-106) concentration.

The apoptotic effect of compound **3** (RC-106) is caspase-dependent, as evidenced by WB assay. Therefore, through this functional assay, we can conclude that **3** (RC-106) is a S2R agonist.

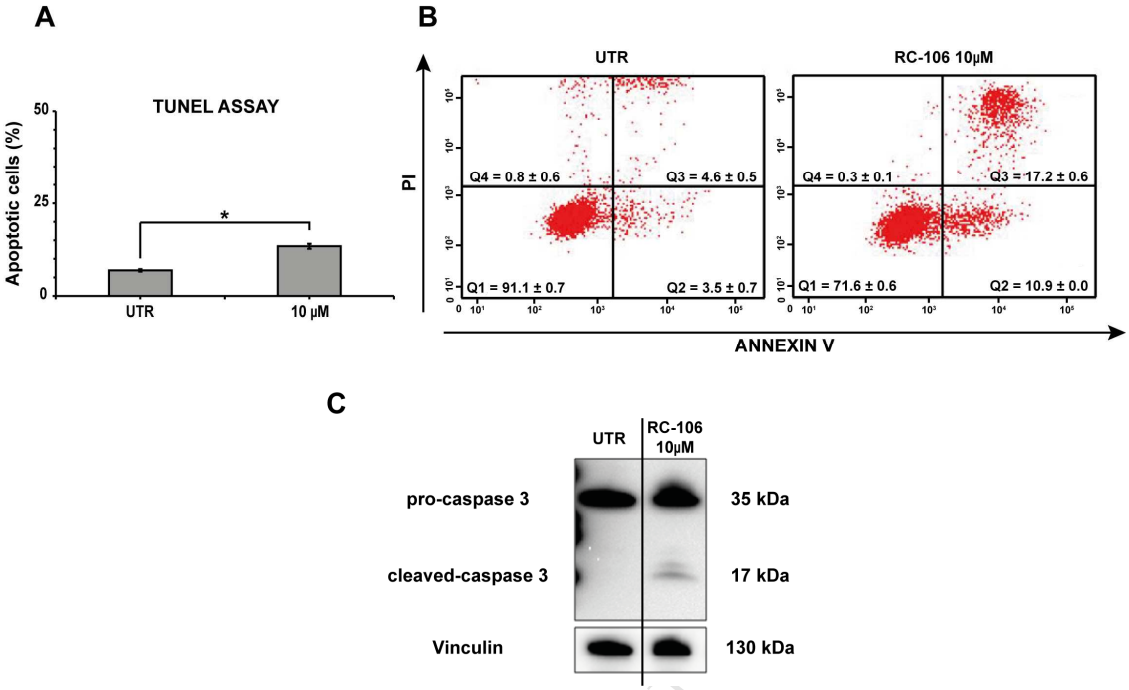

Fig. 10. Apoptosis and apoptotic-related markers analysis in Paca3 cells.

Paca3 cells were exposed to 24 h starvation-condition and to 10 µM compound **3** (RC-106) and the percentage of apoptotic cells was compared in untreated cells (UTR).(A) TUNEL assay: the values are the mean±SD of 3 individual experiments. *$p<0.05$ (B) Representative images of FACS analysis of apoptosis by Annexin V test. (C) WB analysis of apoptotic-related markers. Images are representative of two independent experiments.

3. Discussion

On the basis of recent literature evidences, we hypothesized that pan- SR modulators can evoke anticancer activity. However, the design of new such compounds represents a major challenge, since no structural information is currently available on S2R, which could enable the adoption of effective techniques such as *e.g.*, computer-aided drug design. Notwithstanding these difficulties, and with this new goal in mind, we capitalized our previous work [29c], according to which the presence of a bulky aminic portion seemed to be an important feature in favoring ligand binding to both receptors. Therefore, we designed a new molecular series of aryl-alkyl(alkenyl) 4-benzylamines. The chemical strategy to obtain compounds **1-6**, **9** and **11-12** followed a divergent synthesis, based on the initial preparation of the common β-aminoketone intermediate **A**, easily obtainable

via Michael chemistry (Scheme 1) [29c]. Accordingly, the smooth bromo-lithium exchange on the appropriate aryl bromide afforded the lithiated arene that, upon quenching with β-aminoketone **A**, gave the tertiary alcohols **1-2** in high yields. The subsequent dehydration with trifluoroacetic anhydride under $Cu(OTf)_2$ catalysis conditions [30] afforded a mixture of olefinic regioisomers C3-C4 and the *E* stereoisomer C2-C3. After purification, olefins **3** and **4** were isolated and finally hydrogenated to access the desired amines **5** and **6**. The same strategy was applied for accessing hydroxylated compounds **9** and **11-12**. However, the protection of the aromatic alcohols as TBS ethers (and their corresponding removal) was required to avoid interference with the lithiation step. Concerning the synthetic pathway of **9** and **11-12**, two additional observations are worth at this point: *i*) the lithiation of the protected TBS-bromonaphtols with *n*-BuLi in THF performed better than the *t*-BuLi/Et_2O based method, and *ii*) keeping temperature below -50 °C after quenching with β-aminoketone **A** improved the efficiency of the alcohol synthesis. In the case of racemic compounds, a (semi)preparative chiral high performance liquid chromatography (HPLC) resolution process was performed and the pure enantiomers obtained in amounts sufficient to support a preliminary biological investigation. All compounds showed – *in silico* and *in vitro* - very high/good affinity for the S1R, with K_iS1 values in the range 0.7 – 120 nM (Tables 1, SI1 and SI2, see Supplementary material). Molecular modeling revealed that the main molecular requirements for high S1R affinity (*i.e.*, the instauration of the prototypical salt bridge involving the ligand basic N atom and the carboxylic side chain of Asp126, the encasement of an aromatic portion of the ligand within the hydrophobic S1R cavity lined by residues Ile128, Phe133, Tyr173 and Leu186, and the generation of a set of further stabilizing ligand/receptor π interactions) were all satisfied by the present series of compounds.

Keeping in mind that the purpose of the work was the identification of dual S1R and S2R ligands, compounds **3**, called by us RC-106, and **6** have been selected for a preliminary investigation of their cytotoxic properties, being the molecules in the full series endowed with a good affinity towards both receptor subtypes [**3** (RC-106) K_iS1 = 12.0 ± 5.0 nM; K_iS2 = 22.0 ± 3.0 nM; **6** K_iS1 = 2.1 ± 1.0; K_iS2 = 6.5 ± 3.0]. The preliminary biological evaluation of **3** (RC-106) and **6** were carried out using PaCa3 cell line (MTS assay)

considering the high level of expression of both SRs. For comparative purposes, the effects of siramesine (S2R agonist) and NE100 (S1R antagonist) were also evaluated. Compounds **3** (RC-106) and siramesine showed an interesting antiproliferative activity, both in complete medium and in starvation conditions. Conversely, compound **6** and NE100 showed poor cytotoxic properties and therefore **6** were discarded.

To in depth characterize **3** (RC-106) from a functional point of view, we assessed its S1R agonist/antagonist profile on NGF-induced neuronal differentiation in PC12 cells model [43]. Indeed, it has been reported that S1R agonists, such as (+)-pentazocine, imipramine, fluvoxamine, PRE-084 and RC-33, among the others, potentiate NGF-induced neurite outgrowth in PC12 cells, and that selective S1R antagonist (such as NE-100 and BD1063) significantly attenuate the efficacy of S1R agonists both in the same *in vitro* assay [29c,43-47]. Our results (Fig. 6) clearly show that compound **3** (RC-106) has a S1R antagonist profile.

We then investigated the cytotoxic activity of **3** (RC-106) on a panel of tumor cell lines representative of various cancer types all expressing both SRs. In particular, with regard to S2R, we evaluated PGRMC1 mRNA by RT-PCR as equivalent to S2R expression, even if the actual identity of S2R is still controversial [20,40-54]. When we tested the effect of **3** (RC-106) on actively proliferating tumor cell lines, we observed significant cytotoxicity at concentrations starting from 10 μM in all the cell lines under investigation. Interestingly, **3** (RC-106) showed cytotoxic effect in all the cell lines tested under low proliferation conditions induced by serum deprivation. In particular, our data indicated that a short term starvation (24 hours) enhances the cytotoxic effect of **3** (RC-106), as evidenced by the low IC_{50} values detected and by the low dose of **3** (RC-106) needed to trigger apoptotic mechanism under these conditions**.** This result is also in agreement with recent data from pre-clinical models showing that short term starvation may be able to potentiate the effectiveness of chemotherapy and radiotherapy [55-59]. Several clinical trials are currently studying the effect of fasting or fasting-mimic diets in patients undergoing chemotherapy (NCT01304251, NCT01175837, NCT00936364, NCT01175837, NCT01802346, NCT02126449). Importantly, the apoptotic effect of **3** (RC-106) is caspase-mediated both in normal and in starvation conditions, evidencing the S2R the agonist profile of **3** (RC-106).

To sum up, we identified a S1R antagonist and a S2R agonist exerting an interesting cytotoxic action toward a panel of tumor cell lines (pancreas, breast, prostate and glioblastoma) both in complete medium and under starvation conditions. Our data also suggest that the observed decrease of cell viability is due to an apoptotic process triggered by **3** (RC-106).

4. Conclusion

There is increasing evidence that both S1R and S2R play a significant role in cancer biology, therefore modulator of both SR subtypes could be of high interest for developing novel anti-cancer drugs. In this scenario, we report the design and synthesis of a compound series targeting both SR subtypes with high affinity. Among these, we identified **3** (RC-106), a compound able to induce a strong cytotoxic effect in a wide panel of cancer cell lines, all expressing SRs, both actively proliferating and in low proliferation rate in response to serum deprivation. The antitumor properties of **3** (RC-106) have been observed in all cell lines independently from tumor histotype. In particular, in pancreatic PaCa3 cells, the cell line expressing the highest levels of both receptors, **3** (RC-106) acts as pro-apoptotic drug, inducing a fast triggering of cell death program.

To sum up, **3** (RC-106) exhibited a promising cytotoxic activity on a panel of cancer cell lines of different tumors, representative of various cancer expressing both SRs. This compound could meet the requirements of new-generation drugs to enter into the so-called basket trials, consisting in treating several neoplastic diseases, all characterized by the same molecular alterations, in this case represented by high expression of S1R or S2R or both [60]. Lastly, it has to be underlined that S1R antagonists can be used for alleviating chronic pain, especially in conditions such as neuropathic pain, a pathologic condition that frequently occurs in cancer patients [61-63]. Accordingly, the identification of new, potent pan-sigma receptor modulators will be of great interest, to develop antitumor and analgesic drugs, representing an innovative pharmacological approach for the treatment of cancer patients with advanced disease. Therefore, **3** (RC-106) represents the *hit* compound of a new class of dual-action ligands targeting S1R and S2R potentially useful for the treatment of cancer disease. Moreover, the evaluation of

the antinociceptive properties of **3** (RC-106) is under investigation and will be reported in due course.

5. Experimental section

5.1. General remarks

Reagents and solvents for synthesis were obtained from Aldrich (Italy). Solvents were purified according to the guidelines in Purification of Laboratory Chemicals. Melting points were measured on SMP3 Stuart Scientific apparatus and are uncorrected. Analytical thin-layer-chromatography (TLC) was carried out on silica gel precoated glass-backed plates (Fluka Kieselgel 60 F254, Merck) and on aluminiumoxid precoated aluminium-backed plates (DC-Alufolien Aluminiumoxid 60 F254 neutral, Merck); visualized by ultra-violet (UV) radiation, acidic ammonium molybdate (IV), or potassium permanganate. Flash chromatography (FC) was performed with Silica Gel 60 (particle size 230–400 mesh, purchased from Nova Chimica) and neutral aluminium oxide (particle size 0.05-0.15 mm, purchased from Fluka). Proton nuclear magnetic resonance (NMR) spectra were recorded on a Bruker Avance 500 spectrometer operating at 500 MHz. Proton chemical shifts (δ) are reported in ppm with the solvent reference relative to tetramethylsilane (TMS) employed as the internal standard ($CDCl_3$, δ = 7.26 ppm). The following abbreviations are used to describe spin multiplicity: s = singlet, d = doublet, t = triplet, q = quartet, m = multiplet, br = broad signal, dd = doublet-doublet, td = triplet-doublet. The coupling constant values are reported in Hz. ^{13}C-NMR spectra were recorded on a 500 MHz spectrometer, with complete proton decoupling. Carbon chemical shifts (δ) are reported in ppm relative to TMS with the respective solvent resonance as the internal standard ($CDCl_3$, δ = 77.23 ppm).

UPLC-UV-ESI/MS analysis were carried out on a Acuity UPLC Waters LCQ FLEET system using an ESI source operating in positive ion mode, controlled by ACQUIDITY PDA and 4 MICRO (Waters). Analyses were run on a ACQUITY BEH C18 (50 x 2.1 mm, 1.7 μm) column, at room temperature, with gradient elution (solvent A: water containing 0.1% of formic acid; solvent B: methanol containing 0.1% of formic acid; gradient: 10% B in A to 100% B in 3 minutes, followed by isocratic elution 100% B for

1.5 minutes, return to the initial conditions in 0.2 minutes) at a flow rate of 0.5 mL min^{-1}. All of the final compounds had 95% or greater purity.

Chiral HPLC runs were conducted on a Jasco (Cremella, LC, Italy) HPLC system consisting of PU-1580 pump, 851-AS auto-sampler, and MD-1510 Photo Diode Array (PDA) detector. Experimental data were acquired and processed by Jasco Borwin PDA and Borwin Chromatograph Software. Solvents used for chiral chromatography were HPLC grade and supplied by Carlo Erba (Milan, Italy). Chiral analytical columns: Chiralcel OJ-H (4.6 mm diameter x 150 mm length, dp 5 μm), Chiralpack IC (4.6 mm diameter x 250 mm length, dp 5μm) and Chiralpack IA (4.6 mm diameter x 250 mm length, dp 5 μm). Analytes were detected photometrically at 220 and 254 nm. Unless otherwise specified, sample solutions were prepared dissolving analytes at 1 mg/mL in ethanol and filtered through 0.45 μm PTFE membranes before analysis. The injection volume was 10 μL. Detection was performed at 220 and 254 nm. The retention factor (k) was calculated using the equation $k = (t_R - t_0)/ t_0$, where t_R is the retention time and t0 the dead time (t_0 was considered to be equal to the peak of the solvent front and was taken from each particular run). The enantioselectivity (α) and the resolution factor (Rs) were calculated as follows: $\alpha = k_2 / k_1$ and $Rs = 2 (t_{R2} - t_{R1}) / (w_1 + w_2)$ where t_{R2} and t_{R1} are the retention times of the second and the first eluted enantiomers, and w_1 and w_2 are the corresponding base peak widths. All HPLC analyses were performed at room temperature.

The best conditions found by the screening protocol were applied to a semi-preparative scale-up. The enantiomers of **1**, **2**, **5** and **9** were then completely resolved by a (semi)-preparative process using a Chiralcel OJ-H column (10 mm diameter × 250 mm length, 5 μm), eluting with ethanol (for the compound 2) or methanol (for the compounds 3, 5 and 8) at RT with a flow rate of 2.5 mL/min. Compounds **6** and **12** were resolved on Chiralpak IA (10 mm diameter × 250 mm length, 5 μm) using MeOH at a flow rate of 2.5 mL/min as eluent. The eluate was fractioned according to the UV profile (detection preformed at 220 and 254 nm). The fractions obtained containing the enantiomers were evaporated at reduced pressure. Analytical control of collected fractions was performed using the analytical columns.

Optical rotation values of enantiomeric compounds were measured on a Jasco photoelectric polarimeter DIP 1000 using a 0.5 dm cell and a sodium and mercury lamp (λ = 589 nm, 435 nm); sample concentration values are given in 10^{-2}g mL^{-1} (Table 2)

*5.2. General procedure for the preparation of compounds **1** and **2***

Under nitrogen atmosphere, *tert*-BuLi (2.5 equiv, 1.7 M in pentane) was added dropwise to a -78 °C cooled solution of the appropriate aryl bromide (1.25 equiv) in anhydrous diethyl ether (20 mL). After 20 minutes the reaction was slowly allowed to reach room temperature. The stirring was continued for 1 additional hour and a solution of 4-(4-benzyl-piperidin-1-yl)-butan-2-one (1.0 equiv) in anhydrous diethyl ether (6 mL) was then added dropwise at -78 °C. The reaction mixture was slowly warm to 0 °C, stirred for 3 h and then quenched with water (12 mL); after an acid (pH = 3-4) / base (pH = 8-9) work-up, the combined organic phases were evaporated under vacuum to get the desired compounds.

*5.2.1. 4-(4-benzylpiperidin-1-yl)-2-(naphthalen-2-yl)butan-2-ol, [**1**]:* Yield: 44%; white solid; mp: 105-107 °C; IR (cm^{-1}): 3434, 2918, 1653, 1438, 1156, 1112, 820; ^{1}H-NMR (500 MHz) ($CDCl_3$) δ (ppm): 8.01 (s, 1H), 7.86-7.81 (m, 3H), 7.47-7.45 (m, 3H), 7.28 (t, *J* = 7.8 Hz, 2H), 7.19 (t, *J* = 7.0 Hz, 1H), 7.13 (d, *J* = 7.1 Hz, 2H), 3.19 (d, 1H), 2.54-2.50 (m, 3H), 2.31 (m, 1H), 2.22-2.14 (m, 2H), 1.92 (d, 1H), 1.84 (m, 1H), 1.76 (m, 1H), 1.68 (m, 1H), 1.60 (m, 1H), 1.57 (s, 3H), 1.50 (m, 1H), 1.31 (m, 2H); ^{13}C-NMR (500 MHz) ($CDCl_3$) δ (ppm): 146.3, 140.5,133.3, 132.0, 129.1, 128.2, 128.1, 127.6, 127.4, 125.8, 125.4, 123.8, 123.6, 75.7, 55.1, 54.8, 52.6, 43.1, 37.8, 37.4, 32.6, 32.1, 31.4; UHPLC-ESI-MS: t_R = 2.03, > 99.9% pure (λ = 225 nm), m/z = 374 $[M + H]^+$

*5.2.1.1. (+)-4-(4-benzylpiperidin-1-yl)-2-(naphthalen-2-yl)butan-2-ol, [(+)-**1**]:* White solid; $[\alpha]_D^{20}$= +40.5 (c 0.2, CH_3OH). The IR and NMR spectra are identical to that of **1**. HPLC: t_R = 8.5 min, ee 96.0%.

*5.2.1.2. (-)-4-(4-benzylpiperidin-1-yl)-2-(naphthalen-2-yl)butan-2-ol, [(-)-**1**]:* White solid; $[\alpha]_D^{20}$= -42.3 (c 0.2, CH_3OH). The IR and NMR spectra are identical to that of **1**. HPLC: t_R = 11.1 min, ee 97.0%.

*5.2.2. 4-(4-benzylpiperidin-1-yl)-2-phenylbutan-2-ol, [**2**]:* Yield: 77%; white solid; mp: 90.9-93 °C; IR (cm^{-1}): 3184, 3125, 1602, 1369, 1343, 1156, 846, 699; ^{1}H-NMR (500 MHz) ($CDCl_3$) δ (ppm): 7.45 (d, *J* = 8.9 Hz, 2H), 7.33 (t, *J* = 8.1 Hz, 2H), 7.27 (t, *J* = 7.4 Hz, 2H), 7.21-7.19 (m, 2H), 7.13 (d, *J* = 7.0 Hz, 2H), 3.15 (d, 1H), 2.54 (m, 1H), 2.52 (m, 2H) 2.30 (m, 1H), 2.22 (m, 1H), 2.07 (m, 1H), 1.86 (m, 1H), 1.80 (m, 1H) 1.75 (m, 1H), 1.67 (m, 1H) 1.60 (m, 1H), 1.50 (m, 1H), 1.49 (s, 3H) 1.31 (m, 2H); ^{13}C-NMR (500 MHz) ($CDCl_3$) δ (ppm): 148.9, 140.5, 129.1, 127.9, 128.2, 126.0, 125.8, 125.0, 75.5, 55.1, 54.8, 52.6, 43.1, 37.8, 37.7, 32.6, 32.1, 31.4; UHPLC-ESI-MS: t_R = 1.75, > 97% pure (λ = 210 nm), m/z = 324 $[M + H]^+$

*5.2.2.1. (+)-4-(4-benzylpiperidin-1-yl)-2-phenylbutan-2-ol, [(+)-**2**]:* Yellow oil; $[\alpha]_D^{20}$= +10.5 (c 0.6, CH_3OH). The IR and NMR spectra are identical to that of **2**. HPLC: t_R = 3.4 min, ee 99.9%.

*5.2.2.2. (-)-4-(4-benzylpiperidin-1-yl)-2-phenylbutan-2-ol, [(-)-**2**]:* Yellow oil; $[\alpha]_D^{20}$= -9.2 (c 0.6, CH_3OH). The IR and NMR spectra are identical to that of **2**. HPLC: t_R = 4.2 min, ee 98.0%.

*5.3. General procedure for the preparation of compounds **3** and **4***

Under argon atmosphere trifluoroacetic anhydride (2.0 equiv) was added dropwise to a solution of the tertiary alcohol (1.0 equiv) and copper triflate (2 mol %) in anhydrous dichloromethane (5 mL) cooled to 0 °C. After stirring the reaction a solution of $NaHCO_{3(aq)}$ (5 %) was added. The phases were separated and the organic phase was dried over anhydrous Na_2SO_4 and concentrated under reduced pressure. The obtained crude was purified by alumina (II Brockmann degree) column chromatography (9 *n*-hexane – 1 ethyl acetate).

*5.3.1. (E)-4-benzyl-1-[3-(naphthalen-2-yl)but-2-en-1-yl]piperidine, [**3**]:* Yield: 50%, yellow solid; mp: 221-222 °C; IR (cm^{-1}): 3049-2977, 2926, 2848, 2514, 1597, 1482, 1453-1434, 1287-1157, 1039, 940, 895, 855, 819, 744, 689; ^{1}H-NMR (500 MHz) ($CDCl_3$) δ (ppm): 7.82-7.80 (m, 3H). 7.78 (d, *J* = 9.0 Hz, 1H), 7.61 (d, *J* = 8.6 Hz, 1H),

7.46-7.44 (m, 2H), 7.29 (t, *J* = 7.4 Hz, 2H), 7.20 (t, *J* = 7.1 Hz, 1H), 7.16 (d, *J* = 7.6 Hz, 2H), 6.09 (t, *J* = 6.6 Hz, 1H), 3.22 (d, *J* = 6.5 Hz, 2H), 3.03 (d, 2H) 2.57 (d, *J* = 6.9 Hz, 2 H), 2.16 (s, 3H), 1.98 (t, 2H), 1.68 (d, 2H), 1.57 (m, 1H), 1.38 (m, 2 H); ^{13}C-NMR (500 MHz) ($CDCl_3$) δ (ppm): 140.7, 140.4, 136.9, 133.4, 132.5, 129.1, 128.1, 128.0, 127.6, 127.5, 126.0, 125.7, 125.6, 124.2, 124.1, 57.2, 54.1, 43.2, 37.9, 32.2, 16.1; UHPLC-ESI-MS: t_R = 2.20, >98% pure (λ = 245 nm), m/z = 356 $[M + H]^+$

*5.3.2. (E)-4-benzyl-1-(3-phenylbut-2-en-1-yl)piperidine, [**4**]:* Yield: 42%; yellow solid; mp: 220-222 °C; IR (cm^{-1}): 3085-2979, 2926, 2488, 1641-1580, 1484-1401, 1273-1160, 1038, 943, 835, 765-748, 689; ^{1}H-NMR (500 MHz) ($CDCl_3$) δ (ppm): 7.40 (d, *J* = 7.9, 2H), 7.31-7.28 (m, 4H); 7.24 (m, 1H), 7.19 (t, *J* = 7.6 Hz, 1H), 7.15 (d, *J* = 7.3 Hz, 2H), 5.92 (t, *J* = 6.4 Hz, 1H), 3.16 (d, *J* = 6.5 Hz, 2H), 2.99 (d, 4H), 2.55 (d, *J* = 6.8 Hz, 2H), 2.05 (s, 3H), 1.95 (t, 2H), 1.66 (d, 2H), 1.54 (m, 1H), 1.36 (m, 2H); ^{13}C-NMR (500 MHz) ($CDCl_3$) δ (ppm): 143.3, 140.7, 137.1, 129.1, 128.2, 128.1, 126.9, 125.7, 125.6, 124.9, 57.0, 54.0, 43.2, 37.6, 32.1, 16.1; UHPLC-ESI-MS: t_R = 1.97, > 98% pure (λ = 205 nm), m/z = 306 $[M + H]^+$

*5.4. General procedure for the preparation of compound **5** and **6**.*

To a solution of olefin (1.0 equiv) in absolute ethanol (10 mL) was added a catalytic amount of Pd (0) / C 10% (*p/p*, 0.06 equiv). The suspension was stirred vigorously under hydrogen atmosphere (1 atm). The reaction mixture was then filtered through Celite, using dichloromethane as solvent. The crude was purified by alumina (II Brockmann degree) column chromatography (9 *n*-hexane – 1 ethyl acetate).

*5.4.1. 4-benzyl-1-[3-(naphthalen-2-yl)butyl]piperidine, [**5**]:* Yield: 56%, yellow oil; IR (cm^{-1}): 3025, 2924, 2508, 1631, 1602, 1542, 1496, 1453; ^{1}H-NMR (500 MHz) ($CDCl_3$) δ (ppm): 7.79-7.77 (t, *J* = 8.7 Hz, 3H), 7.59 (s, 1H), 7.45-7.42 (m, 2H), 7.32 (d, *J* = 8.8 Hz, 1H), 7.25 (m, 2H), 7.17 (m, 1H), 7.08 (m, 2H), 3.30 (broad peak, 2H), 2.90 (m, 1H), 2.76 (m, 1H), 2.55 (d, *J* = 7.4 Hz, 2H), 2.46 (m, 1H), 2.27-2.13 (m, 4H), 1.82-1.71 (m, 4H), 1.59 (m, 1H), 1.36 (d, J = 6.5 Hz, 3H); ^{13}C-NMR (500 MHz) ($CDCl_3$) δ (ppm): 142.4, 139.3, 133.4, 132.3, 128.9, 128.5, 128.3, 127.6, 127.5, 126.1, 125.5, 125.3, 124.8, 56.1,

52.4, 41.9, 38.3, 36.5, 31.8, 29.1, 22.7; UHPLC-ESI-MS: t_R = 2.17, > 97% pure (λ = 220 nm), m/z = 358 $[M + H]^+$

*5.4.1.1. (+)-4-benzyl-1-(3-(naphthalen-2-yl)butyl)piperidine, [(+)-**5**]:* Yellow oil; $[\alpha]_D^{20}$= +6.1 (c 0.2, CH_3OH). The IR and NMR spectra are identical to that of **5**. HPLC: t_R = 7.7 min, ee 95.0%.

*5.4.1.2. (-)-4-benzyl-1-(3-(naphthalen-2-yl)butyl)piperidine, [(-)-**5**]:* Yellow oil; $[\alpha]_D^{20}$= -6.3 (c 0.2, CH_3OH). The IR and NMR spectra are identical to that of **5**. HPLC: t_R = 9.0 min, ee 95.0%.

*5.4.2. 4-benzyl-1-(3-phenylbutyl)piperidine, [**6**]:* Yield: 47%, yellow oil; IR (cm^{-1}): 3682, 3019, 2929, 2856, 2434, 2400, 1230; ^{1}H-NMR (500 MHz) ($CDCl_3$) δ (ppm): 7.28-7-27 (m, 4H), 7.17 (m, 4H), 7.13 (d, *J* = 7.0 Hz, 2H), 2.86 (broad peak, 2H), 2.71 (m, 1H), 2.52 (d, *J* = 6.6 Hz, 2H), 2.26 (m, 1H), 2.14 (m, 1H), 1.87-1.72 (m, 4H), 1.61 (d, 2H), 1.49 (m, 1H), 1.29 (m, 2H), 1.24 (d, *J* = 7.3 Hz, 3H); ^{13}C-NMR (500 MHz) ($CDCl_3$) δ (ppm): 147.3, 140.7, 129.1, 128.3, 128.1, 126.9, 125.9, 125.7, 57.3, 54.1, 53.9, 43.2, 38.4, 37.9, 35.4, 32.1, 22.6; UHPLC-ESI-MS: t_R = 1.92, > 97% pure (λ = 200 nm), m/z = 308 $[M + H]^+$

*5.4.2.1. (+)-4-benzyl-1-(3-phenylbutyl)piperidine, [(+)-**6**]:* Yellow oil; $[\alpha]_D^{20}$= +8.2 (c 0.3, CH_3OH). The IR and NMR spectra are identical to that of **6**. HPLC: t_R = 3.7 min, ee 99.9%.

*5.4.2.2. (-)-4-benzyl-1-(3-phenylbutyl)piperidine, [(-)-**6**]:* Yellow oil; $[\alpha]_D^{20}$= -8.3 (c 0.3, CH_3OH). The IR and NMR spectra are identical to that of **6**. HPLC: t_R = 5.3 min, ee 99.9%.

*5.5. (6-bromonaphthalen-2-yloxy)-tert-butyldimethtyl-silane, [**7**]*

Under argon atmosphere 6-bromo-2-naphthol (1.0 equiv), imidazole (1.0 equiv) and *tert*-butyldimethylsilyl chloride (1.2 equiv) were solubilized in anhydrous dimethylformamide (20 mL). After stirring the solution overnight, the reaction mixture was extracted by

dichloromethane (x 2) and brine (x 5). The organic phase was dried over Na_2SO_4, and concentrated under reduced pressure. The crude was purified by column chromatography (10 *n*-hexane).

Yield: 90%, white solid; mp: 62-64 °C; IR (cm^{-1}): 3743, 2954, 1735, 1653, 1560, 1470, 1256, 1062; ^{1}H-NMR (500 MHz) ($CDCl_3$) δ (ppm): 7.92 (s, 1H), 7.64 (d, *J* = 8.9 Hz, 1H), 7.57 (d, *J* = 8.9 Hz, 1H), 7.48 (dd, *J* = 9.2 and 2.3 Hz, 1H), 7.16 (ds, *J* = 2.4 Hz, 1H), 7.10 (dd, *J* = 8.5 and 2.2 Hz, 1H), 1.02 (s, 9H), 0.25 (s, 6H); ^{13}C-NMR (500 MHz) ($CDCl_3$) δ (ppm): 153.8, 133.1, 130.2, 129.6, 129.4, 128.4, 128.3, 123.1, 117.3, 114.9, 25.7, 18.2, -4.4; ESI-MS: m/z = 338 $[M + H]^+$

*5.6. 4-(4-benzylpiperidin-1-yl)-2-[6-(tert-butyldimethyl-silanoloxy)-naphtalen-2-yl]-butan-2-ol, [**8**]*

Compound **7** (1.5 equiv) was dissolved in anhydrous tetrahydrofuran (5 mL) under argon atmosphere. The solution was cooled to -78 °C, then was added dropwise *n*-butyl-lithium (4.4 equiv, 2.5 M in *n*-hexane). After 20 minutes, the temperature was increased up to -50 °C and a solution of 4-(4-benzyl-piperidin-1-yl)-butan-2-one (1.0 equiv) in anhydrous tetrahydrofuran (5.0 mL) was added dropwise. The reaction mixture was stirred for 1.5 h, keeping the temperature below -50 °C. The solution was quenched with 10 mL of saturated solution of $NH_4Cl_{(aq)}$ and extracted with Et_2O. The organic phase was dried over Na_2SO_4. The solvent was removed under reduced pressure and the crude was purified by alumina (II Brockmann degree) column chromatography (8 *n*-hexane – 2 ethyl acetate).

Yield: 63%; bright yellow oil; IR (cm^{-1}): 3336, 3026, 2926, 2856, 2349, 2310, 1603, 1496, 1471, 1453, 1371, 1260; ^{1}H-NMR (500 MHz) ($CDCl_3$) δ (ppm): 7.92 (s, 1H), 7.72 (d, *J* = 9.1 Hz, 1H), 7.65 (d, *J* = 8.6 Hz, 1H), 7.42 (d, *J* = 8.6 Hz, 1H), 7.27 (m, 2H), 7.18 (t, *J* = 7.7 Hz, 2H), 7.12 (t, *J* = 8.6 Hz, 2H), 7.06 (dd, *J* = 8.4 and 1.8 Hz, 1H), 3.18 (broad peak, 1H), 3.02 (broad peak, 1H), 2.61 (broad peak, 1H), 2.53 (m, 2H), 2.31 (d, 1H), 2.12 (t, 1H), 1.92-1.86 (m, 2H), 1.75 (m, 1H), 1.65-1.63 (m, 2H), 1.54 (s, 3H), 1.51 (m, 1H), 1.29 (m, 2H), 1.02 (s, 9H), 0.24 (s, 6H); ^{13}C-NMR (500 MHz) ($CDCl_3$) δ (ppm):

153.2, 144.2, 140.5, 133.1, 129.4, 129.1, 129.0, 128.2, 126.4, 125.8, 124.1, 123.3, 122.0, 114.5, 75.6, 55.1, 54.7, 54.2, 53.7, 52.6, 43.1, 37.8, 37.4, 32.5, 32.1, 31.4, 25.7, 18.2, -4.3; APCI-MS: m/z = 504 $[M + H]^+$

*5.7. (E)-4-benzyl-1-{3-[6-(tert-butyldimethyl-silanyloxy)-naphthalen-2-yl]-but-2-en-1-yl}-piperidine, [**10**].*

Under argon atmosphere trifluoroacetic anhydride (2.0 equiv) was added dropwise to a solution of compound **8** (1.0 equiv) and copper triflate (2 mol %) in anhydrous dichloromethane (5 mL) cooled to 0 °C. After stirring the reaction a solution of $NaHCO_{3(aq)}$ (5 %) was added. The phases were separated and the organic phase was dried over anhydrous Na_2SO_4 and concentrated under reduced pressure. The obtained crude was purified by alumina (II Brockmann degree) column chromatography (9 *n*-hexane – 1 ethyl acetate).

Yield: 61%; yellow solid; mp: 102-104 °C; IR (cm^{-1}): 3027, 2926, 2856, 2801, 2349, 1597, 1497, 1478, 1374, 1318, 1257; ^{1}H-NMR (500 MHz) ($CDCl_3$) δ (ppm): 7.74 (s, 1H), 7.69 (d, *J* = 9.0 Hz, 1H), 7.63 (d, *J* = 8.9 Hz, 1H), 7.56 (d, *J* = 8.7 Hz, 1H), 7.28 (m, 2H), 7.19-7.15 (m, 4H), 7.06 (d, *J* = 9.1 Hz, 1H), 6.04 (t, *J* = 6.7 Hz, 1H), 3.21 (d, 2H), 3.02 (broad peak, 2H), 2.56 (d, *J* = 7.0 Hz, 2H), 2.13 (s, 3H), 1.97 (broad peak, 2H), 1.68 (broad peak, 2H), 1.55 (broad peak, 1H), 1.36 (m, 2H), 1.02 (s, 9H), 0.25 (s, 6H); ^{13}C-NMR (500 MHz) ($CDCl_3$) δ (ppm): 153.4, 140.7, 138.5, 136.9, 133.7, 129.4, 129.1, 128.1, 126.4, 125.7, 125.0, 124.5, 123.9, 122.2, 114.7, 57.2, 54.1, 43.2, 37.9, 32.2, 25.7, 18.2, 16.1, -4.4; ESI-MS: m/z = 486 $[M + H]^+$

*5.8. General procedure for the preparation of compounds **9** and **11***

Tetra-N-butylammonium fluoride (1.5 equiv, 1.0 M in tetrehydrofuran) was added dropwise to a solution of compounds **8** and **10** (1.0 equiv) in anhydrous dichloromethane (5.0 mL), at 0 °C, in argon atmosphere. After 2 h the reaction mixture was extracted by a solution of $NaHCO_3$ (5%). In the case of compound **9**, the crude was purified by column chromatography (9 dichloromethane – 1 methanol – 0.1% NH_3 in methanol); on the

contrary for compound **11**, it was been enough to do a precipitation of the solid impurities using methanol.

*5.8.1. 6-[4-(4-benzylpiperidin-1-yl)-2-hydroxybutan-2-yl]naphthalen-2-ol, [**9**]:* Yield: 64%; yellow oil; IR (cm^{-1}): 3452, 2925, 1633, 1605, 1560, 1454, 1381; ^{1}H-NMR (500 MHz) ($CDCl_3$) δ (ppm): 7.91 (s, 1H), 7.72 (d, *J* = 8.4 Hz, 1H), 7.60 (d, *J* = 8.4 Hz, 1H), 7.40 (d, *J* = 8.8 Hz, 1H), 7.25 (t, *J* = 6.9 Hz, 2H), 7.18-7.14 (m, 3H), 7.07 (d, *J* = 8.0 Hz, 2H), 3.20 (broad peak, 1H), 2.61 (broad peak, 1H), 2.46 (d, *J* = 6.5 Hz, 2H), 2.34 (m, 2H), 2.18 (m, 1H), 1.96 (broad peak, 1H), 1.88 (broad peak, 1H), 1.80 (broad peak, 1H), 1.66 (broad peak, 2H), 1.59 (s, 1H), 1.49 (broad peak, 1H), 1.34 (broad peak, 2H); ^{13}C-NMR (500 MHz) ($CDCl_3$) δ (ppm): 154.0, 143.0, 140.3, 133.3, 129.8, 129.0, 128.5, 128.2, 126.2, 125.8, 124.1, 123.4, 118.3, 109.2, 75.8, 55.0, 54.7, 52.6, 42.9, 37.6, 37.4, 31.7, 31.3; UHPLC-ESI-MS: t_R = 1.68, > 97% pure (λ = 230 nm), m/z = 390 $[M + H]^+$

*5.8.1.1. (+)-6-[4-(4-benzylpiperidin-1-yl)-2-hydroxybutan-2-yl]naphthalen-2-ol, [(+)-**9**]:* Yellow oil; $[\alpha]_D^{20}$= +24.2 (c 0.1, CH_3OH). The IR and NMR spectra are identical to that of **9**. HPLC: t_R = 4.0 min, ee 99.9%.

*5.8.1.2. (-)-6-[4-(4-benzylpiperidin-1-yl)-2-hydroxybutan-2-yl]naphthalen-2-ol, [(-)-**9**]:* Yellow oil; $[\alpha]_D^{20}$= -24.8 (c 0.1, CH_3OH). The IR and NMR spectra are identical to that of **9**. HPLC: t_R = 5.0 min, ee 99.9%.

*5.8.2. (E)-6-[4-(4-benzylpiperidin-1-yl)but-2-en-2-yl]naphthalen-2-ol, [**11**]:* Yield: 64%; bright yellow solid; mp: 157-159 °C; IR (cm^{-1}): 3629, 2926, 2854,2349, 1601, 1454; ^{1}H-NMR (500 MHz) ($CDCl_3$) δ (ppm): 7.50 (s, 1H), 7.44 (d, *J* = 8.7 Hz, 1H), 7.28 (t, *J* = 8.1 Hz, 2H), 7.19 (t, *J* = 8.0 Hz, 1H), 7.15-7.11 (t, *J* = 7.8 Hz, 2H), 7.03-7.01 (m, 3H), 6.89 (ds, 1H), 5.89 (t, *J* = 7.2 Hz, 1H), 3.28 (ds, 2H), 3.21 (ds, 2H), 2.57 (d, *J* = 7.5 Hz, 2H), 2.13 (m, 2H), 2.12 (s, 3H), 1.74 (m, 2H), 1.63 (m, 1H), 1.53 (m, 2H); ^{13}C-NMR (500 MHz) ($CDCl_3$) δ (ppm): 154.5, 140.4, 136.7, 134.0, 130.0, 129.1, 128.2, 128.0, 125.9, 124.0, 123.7, 122.7, 119.2, 109.9, 56.8, 53.9, 42.9, 37.8, 31.3, 15.7; UHPLC-ESI-MS: t_R = 1.92, > 97% pure (λ = 245 nm), m/z = 372 $[M + H]^+$

*5.9. 6-[4-(4-benzylpiperidin-1-yl)butan-2-yl]naphthalen-2-ol, [**12**]:*

To a solution of compound **11** (1.0 equiv) in absolute ethanol (10 mL) was added a catalytic amount of Pd (0) / C 10% (*p/p*, 0.06 equiv). The suspension was stirred vigorously under hydrogen atmosphere (1 atm). The reaction mixture was then filtered through Celite, using dichloromethane as solvent. The crude was purified by column chromatography (9 dichloromethane – 1 methanol – 0.1% NH_3 in methanol).

Yield: 39%; yellow oil; IR (cm^{-1}): 3297, 2924, 2349, 2309, 1604, 1453, 1376, 1269; ^{1}H-NMR (500 MHz) ($CDCl_3$) δ (ppm): 7.42 (d, *J* = 9.0 Hz, 1H), 7.37 (s, 1H), 7.24 (t, 2H), 7.17 (d, *J* = 8.0 Hz, 1H), 7.17 (m, 1H), 7.06 (m, 3H), 6.98 (d, *J* = 9.0 Hz, 1H), 6.81 (s, 1H), 3.26 (broad peak, 1H), 3.10 (broad peak, 1H), 2.73 (m, 1H), 2.50-2.49 (broad peak, 4H), 2.14-2.12 (m, 2H), 2.04 (m, 2H), 1.67 (m, 2H), 1.60-1.54 (m, 3H), 1.28 (overlapped peak, 3H); ^{13}C-NMR (500 MHz) ($CDCl_3$) δ (ppm): 154.6, 139.5, 133.6, 129.0, 128.3, 126.8, 126.0, 125.1, 125.0, 118.7, 109.2, 56.5, 53.7, 52.9, 42.3, 38.1, 37.0, 33.2, 30.0, 22.9; UHPLC-ESI-MS: t_R = 1.86, > 95% pure (λ = 230 nm), m/z = 374 $[M + H]^+$

*5.9.1. (+)-6-[4-(4-benzylpiperidin-1-yl)butan-2-yl]naphthalen-2-ol, [(+)-**12**]:* Yellow oil; $[\alpha]_D^{20}$= +11.8 (c 0.3, CH_3OH). The IR and NMR spectra are identical to that of **12**. HPLC: t_R = 4.9 min, ee 99.9%.

*5.9.2. (-)-6-[4-(4-benzylpiperidin-1-yl)butan-2-yl]naphthalen-2-ol, [(-)-**12**]:* Yellow oil; $[\alpha]_D^{20}$= -12.0 (c 0.3, CH_3OH). The IR and NMR spectra are identical to that of **12**. HPLC: t_R = 5.7 min, ee 99.9%.

5.10. Molecular modeling

The optimized structures of selected compounds were docked into the putative binding pockets for the S1R by applying a consolidated procedure [29d,31a,32-35,64]. The resulting docked conformations for each complex were clustered and visualized; then, for each compound, only the molecular conformation satisfying the combined criteria of having the lowest (i.e., more favorable) energy and belonging to a highly populated cluster was selected to carry for further modeling. The ligand/receptor complexes obtained from the docking procedure was further refined in Amber 14 [65] using the

quenched molecular dynamics (QMD) method, as previously described [29d,31a,32-35,64]. According to QMD, the best energy configuration of each complex resulting from this step was subsequently solvated by a cubic box of TIP3P [66] water molecules extending at least 10 Å in each direction from the solute. The system was neutralized and the solution ionic strength was adjusted to the physiological value of 0.15 M by adding the required amounts of Na^+ and Cl^- ions. Each solvated system was relaxed by 500 steps of steepest descent followed by 500 other conjugate-gradient minimization steps and then gradually heated to a target temperature of 300 K in intervals of 50 ps of NVT MD, using a Verlet integration time step of 1.0 fs. The Langevin thermostat was used to control temperature, with a collision frequency of 2.0 ps^{-1} The protein was restrained with a force constant of 2.0 kcal/(mol Å), and all simulations were carried out with periodic boundary conditions. Subsequently, the density of the system was equilibrated via MD runs in the isothermal-isobaric (NPT) ensemble, with isotropic position scaling and a pressure relaxation time of 1.0 ps for 50 ps with a time step of 1 fs. All restraints on the protein atoms were then removed, and each system was further equilibrated using NPT MD runs at 300 K, with a pressure relaxation time of 2.0 ps. Three equilibration steps were performed, each 2 ns long and with a time step of 2.0 fs. To check the system stability, the fluctuations of the rmsd of the simulated position of the backbone atoms of the receptor with respect to those of the initial protein were monitored. All chemophysical parameters and rmsd values showed very low fluctuations at the end of the equilibration process, indicating that the systems reached a true equilibrium condition. The equilibration phase was followed by a data production run consisting of 40 ns of MD simulations in the canonical (NVT) ensemble. Only the last 20 ns of each equilibrated MD trajectory were considered for statistical data collections. A total of 1000 trajectory snapshots were analyzed the each ligand/receptor complex. The binding free energy, ΔG_{bind}, between the ligands and the sigma1 receptor was estimated by resorting to the MM/PBSA approach implemented in Amber 14. According to this well validated methodology [36], the free energy was calculated for each molecular species (complex, receptor, and ligand), and the binding free energy was computed as the difference:

$$\Delta G_{bind} = G_{complex} - (G_{receptor} + G_{ligand}) = \Delta E_{MM} + \Delta G_{sol} - T\Delta S$$

in which ΔE_{MM} represents the molecular mechanics energy, ΔG_{sol} includes the solvation free energy and $T\Delta S$ is the conformational entropy upon ligand binding. The per residue decomposition of the enthalpic term of ΔG_{bind} was performed exploiting the equilibrated MD trajectory of each given compound/receptor complex. This analysis was carried out using the MM/GBSA approach [67,68], and was based on the same snapshots used in the binding free energy calculation. All simulations were carried out using the Pmemd modules of Amber 14, running on the MOSE CPU/GPU calculation cluster.

5.11. Binding assays

5.11.1. Materials

Guinea pig brains for the S1R binding assays were commercially available (Harlan–Winkelmann, Borchen, Germany). Homogenizer: Elvehjem Potter (B. Braun Biotech International, Melsungen, Germany) and Soniprep 150, MSE, London, UK). Centrifuges: Cooling centrifuge model Rotina 35R (Hettich, Tuttlingen, Germany) and High-speed cooling centrifuge model Sorvall RC-5C plus (Thermo Fisher Scientific, Langenselbold, Germany). Multiplates: standard 96-well multiplates (Diagonal, Muenster, Germany). Shaker: self-made device with adjustable temperature and tumbling speed (scientific workshop of the institute). Vortexer: Vortex Genie 2 (Thermo Fisher Scientific, Langenselbold, Germany). Harvester: MicroBeta FilterMate-96 Harvester. Filter: Printed Filtermat Type A and B. Scintillator: Meltilex (Type A or B) solid-state scintillator. Scintillation analyzer: MicroBeta Trilux (all PerkinElmer LAS, Rodgau-Jügesheim, Germany). Chemicals and reagents were purchased from various commercial sources and were of analytical grade.

5.11.2. Preparation of membrane homogenates from guinea pig brain cortex

Five guinea pig brains were homogenized with the potter (500–800 rpm, 10 up-and-down strokes) in six volumes of cold 0.32m sucrose. The suspension was centrifuged at 1200 g for 10 min at 4°C. The supernatant was separated and centrifuged at 23500 *g* for 20 min at 4°C. The pellet was resuspended in 5–6 volumes of buffer (50 mm Tris, pH 7.4) and centrifuged again at 23500 *g* (20 min, 4 8C). This procedure was repeated twice. The

final pellet was resuspended in 5–6 volumes of buffer and frozen (-80°C) in 1.5 mL portions containing ~1.5 (mg protein)mL^{-1}.

5.11.3. Protein determination

The protein concentration was determined by the method of Bradford[S2] modified by Stoscheck.[S3] The Bradford solution was prepared by dissolving 5 mg of Coomassie Brilliant Blue G 250 in 2.5 mL EtOH (95% v/v). Deionized H_2O (10 mL) and phosphoric acid (85% w/v, 5 mL) were added to this solution, and the mixture was stirred and filled to a total volume of 50 mL with deionized water. Calibration was carried out using bovine serum albumin as a standard in nine concentrations (0.1, 0.2, 0.4, 0.6, 0.8, 1.0, 1.5, 2.0, and 4.0 mg mL^{-1}). In a 96-well standard multiplate, 10 mL of the calibration solution or 10 mL of the membrane receptor preparation were mixed with 190 mL of the Bradford solution. After 5 min, the UV absorption of the protein–dye complex at l=595 nm was measured with a plate reader (Tecan Genios, Tecan, Crailsheim, Germany).

5.11.4. General protocol for binding assays

The test compound solutions were prepared by dissolving ~10 mmol (usually 2–4 mg) of test compound in DMSO so that a 10 µM stock solution was obtained. To obtain the required test solutions for the assay, the DMSO stock solution was diluted with the respective assay buffer. The filtermats were presoaked in 0.5% aqueous polyethylenimine solution for 2 h at RT before use. All binding experiments were carried out in duplicate in 96-well multiplates. The concentrations given are the final concentrations in the assay. Generally, the assays were performed by addition of 50 µL of the respective assay buffer, 50 µL test compound solution at various concentrations (10^{-5}, 10^{-6}, 10^{-7}, 10^{-8}, 10^{-9} and 10^{-10}M), 50 µL of corresponding radioligand solution, and 50 µL of the respective receptor preparation into each well of the multiplate (total volume 200 µL). The receptor preparation was always added last. During the incubation, the multiplates were shaken at a speed of 500–600 rpm at the specified temperature. Unless otherwise noted, the assays were terminated after 120 min by rapid filtration using the harvester. During the filtration each well was washed five times with 300 mL of water. Subsequently, the filtermats were dried at 95°C. The solid scintillator was melted on the dried filtermats at 95°C for 5 min.

After solidifying of the scintillator at RT, the trapped radioactivity in the filtermats was measured with the scintillation analyzer. Each position on the filtermat corresponding to one well of the multiplate was measured for 5 min with the [^{3}H]-counting protocol. The overall counting efficiency was 20%. The IC50 values were calculated with GraphPad Prism 3.0 (GraphPad Software, San Diego, CA, USA) by nonlinear regression analysis. The IC50 values were subsequently transformed into Ki values using the equation of Cheng and Prusoff. The Ki values are given as mean value ±SEM from three independent experiments.

5.11.5. S1R binding assay

The assay was performed with the radioligand [^{3}H](+)-pentazocine (22.0 Ci mmol^{-1}; PerkinElmer). The thawed membrane preparation of guinea pig brain cortex (~100 mg protein) was incubated with various concentrations of test compounds, 2 nM [^{3}H](+)-pentazocine, and Tris buffer (50 mM, pH 7.4) at 37°C. The nonspecific binding was determined with 10 mM unlabeled (+)-pentazocine. The Kd value of (+)-pentazocine is 2.9 nM.

5.11.6. S2R binding assay

The assay was performed using 150 µg of rat liver homogenate were incubated for 120 min at room temperature with 3 nM [^{3}H]-DTG (Perkin–Elmer, specific activity 58.1 Ci mmol^{-1}) in 50 mM Tris–HCl, pH 8.0, 0.5 mL final volume. (+)-pentazocine (100 nM) and haloperidol (10 µM) were used to mask S1R and to define non-specific binding, respectively.

5.12. Cell lines

PC12 cells were grown in RPMI 1640 (Mediatech, Manassas, VA) supplemented with 10% heat inactivated horse serum (HS) and 5% fetal bovine serum (FBS) (Biochrom) 1% Glutamax, 1% penicillin/streptomycin (pen/strep). Cell differentiation was induced by exposure to a medium containing RPMI 1640 supplemented with 0.5% HS, Glutamax 1%, pen/strep 1% and NGF 2.5ng/ml. PRE-084 and BD-1063 were prepared at 10 mM stock solutions in apyrogenic water. Pancreatic adenocarcinoma Capan-2 and PaCa3,

breast adenocarcinoma MDA-MB 231 and SUM 159 cell line and prostatic adenocarcinoma PC3 cell lines were grown in culture medium composed of DMEM/Ham's F12 (1:1) (Euroclone) supplemented with fetal calf serum (FCS) (10%) (Euroclone), glutamine (2 mM) (Euroclone) and insulin (10 µg/ml) (Sigma-Aldrich, St. Louis, MO, USA). Glioblastoma cell line U87 was grown in EMEM culture medium (Euroclone) supplemented with FCS (10%) and glutamine (2mM). Prostatic adenocarcinoma cell line LNCaP was grown in RPMI culture medium (Euroclone) supplemented with FCS (10%) and glutamine (2mM). Serum restriction was done by incubating cells in low glucose culture medium without FCS for 24 h. All cell lines were purchased by the American Type Culture Collection (ATCC) except for SUM 159 that was purchased from Amsterand plc (Detroit, MI, USA).

All experiments were performed on cells in the exponential growth phase and checked periodically for mycoplasma contamination by MycoAlert™ Mycoplasma Detection Kit (Lonza, Basel, Switzerland).

5.13. Cytotoxicity test

5.13.1. MTS Assay

CellTiter 96® AQueous One Solution Cell Proliferation Assay (Promega, Milan, Italy) was used on cells seeded onto a 96-well plate at a density of 3×10^3 cells per well. The effect of the drugs was evaluated after 24 h of continued exposure. Three independent experiments were performed in octuplicate. The optical density (OD) of treated and untreated cells was determined at a wavelength of 490 nm using a plate reader. Dose response curves were created by Excel software. IC_{50} values were determined graphically from the plot.

5.13.2. Flow Cytometry

Flow cytometric analysis was performed using a FACS Canto flow cytometer (Becton Dickinson, San Diego, CA). Data acquisition and analysis were performed using FACSDiva software (Becton Dickinson). Samples were run in triplicate and 10,000 events were collected for each replicate.

5.13.3. Annexin-V assay

After exposure to compound, medium was removed and cell were detached by tripsinization, washed once in PBS 1X and incubated with 25µl/ml Annexin V-FITC in binding buffer (Affimetrix eBioscience, San Diego, USA) for 15 min at 37°C in a humidified atmosphere in the dark. Cells were then washed in PBS and suspended in binding buffer.

Immediately before flow cytometric analysis, propidium iodide was added to a final concentration of 5 µg/ml to discriminate between apoptotic (Ann-V positive and PI positive or PI negative) and necrotic cells (Ann-V negative and PI positive).

5.13.4. TUNEL assay

Cells were fixed in 1% formaldehyde in PBS on ice for 15 min, suspended in 70% ice cold ethanol and stored overnight at 20°C. Cells were then washed twice in PBS and re-suspended in PBS containing 0.1% Triton X-100 for 5 min at 48C. Thereafter, samples were incubated in 50µl of solution containing TdT and FITC conjugated dUTP deoxynucleotides 1:1 (Roche Diagnostic GmbH, Mannheim, Germany) in a humidified atmosphere for 90 min at 37°C in the dark, washed in PBS, counterstained with propidium iodide (2.5 µg/ml, MP Biomedicals, Verona, Italy) and RNAse (10 kU/ml, Sigma–Aldrich) for 30 min at 48°C in the dark and analyzed by flow cytometry.

5.13.5. Western blot

Cell proteins were extracted with M-PER Mammalian Protein Extraction Reagent (Thermo Fisher Scientific) supplemented with Halt Protease Phosphatase Inhibitor Cocktail (Thermo Fisher Scientific). Mini-PROTEANTGX™ precast gels (4–20%) (BIO-RAD) were run using Mini-PROTEAN Tetra electrophoresis cells and then electroblotted by Trans-BlotTurbo™ Mini PVDF Transfer Packs (BIORAD). The unoccupied membrane sites were blocked with T-TBS 1X (Tween 0.1%) and 5% non-fat dry milk to prevent nonspecific binding of antibodies and probed with specific primary antibodies overnight at 4 °C. This was followed by incubation with the respective secondary antibodies. The antibody-antigen complexes were detected with Immun-Star™ WesternC™ kit (BIO-RAD).

The following primary antibodies were used: anti-caspase-3 (Cell Signaling Technology, Inc., Celbio, Pero, Milan, Italy). Ant-vinculin (sc-5573) from Santa Cruz Biotechnology was used as housekeeping. Quantity One Software was used for analysis

5.14. Real time RT-PCR

Total cellular RNA was extracted using TRIzol reagent (Life technologies) in accordance with manufacturer's instruction and quantified using the Nanodrop MD-1000 spectrophotometer system. Reverse transcription reactions were performed in 20 µL of nuclease free water containing 400 ng of total RNA using iScript cDNA Synthesis kit (Bio-Rad Laboratories, Hercules, CA). Real-Time PCR was run using 7500 Fast Real-Time PCR system (Applied Biosystems) and TaqMan assays to detect the expression of SIGMAR1 and PGRMC1 genes.

Reactions were carried out in triplicate at a final volume of 20 µL containing 40 ng of cDNA template, TaqMan universal PCR Master Mix (2X), and selected TaqMan assays (20X). Samples were maintained at 50°C for 2 minutes, then at 95°C for 10 minutes followed by 40 amplification cycles at 95°C for 15 seconds, and at 60°C for 30 seconds.

The amount of mRNA was normalized to the endogenous genes GAPDH and HPRT-1.

5.15. Statistical analysis

All statistical analyses were done using standard software packages GraphPad Prism (GraphPad Software, San Diego California USA, version 5.0). The comparison between groups was performed by applying the Student "t" test for 2-group comparisons or one-way ANOVA followed by appropriate post hoc tests for multiple comparisons. p-values lower than 0.05 were considered statistically significant.

Acknowledgement

The Authors gratefully acknowledge Ilaria Rocchio for the experimental support and Stefania Brambilla for UHPLC-ESI-MS analysis.

References

[1] S.B. Hellewell, A. Bruce, G. Feinstein, J. Orringer, W. Williams, W.D. Bowen. Rat liver and kidney contain high densities of sigma 1 and sigma 2 receptors: characterization by ligand binding and photoaffinity labeling, Eur. J. Pharmacol. 268 (1994) 9–18.

[2] R. Quirion, W. Bowen, Y. Itzhak, J.L. Junien, J.M. Musacchio, R.B. Rothman, T.P. Su, S.W. Tam, D.P. Taylor. A proposal for the classification of sigma binding sites, Trends Pharmacol. Sci. 13 (1992) 85–86.

[3] M. Hanner, F.F. Moebius, A. Flandofer, H.G. Knaus, J. Striessnig, E. Kempner, H. Glossmann. Purification, molecular cloning, and expression of the mammalian sigma1-binding site, Proc. Natl. Acad. Sci. U.S.A. 93 (1996) 8072–8077.

[4] W.D. Bowen. Sigma receptors: Recent advances and new clinical potentials, Pharmaceutica Acta Helvetiae 74 (2000) 211-218.

[5] S. Collina, R. Gaggeri, A. Marra, A. Bassi, S. Negrinotti, F. Negri, D. Rossi. Sigma receptor modulators: a patent review, Exp. Opin. Ther. Patent 23 (2013) 597-613.

[6] S.Y. Tsai, T. Hayashi, T. Mori, T.P. Su. Sigma-1 receptor chaperones and diseases, Cent. Nerv. Syst. Agents Med. Chem. 9 (2009) 184–189.

[7] V.L. Phan, G. Alonso, F. Sandillon, A. Privat, T. Maurice. Therapeutic potentials of sigma1 (sigma 1) receptor ligands against cognitive deficits in aging, Soc. Neurosci. Abstr. 26 (2000) 2172.

[8] A. Marra, D. Rossi, L. Pignataro, C. Bigogno, A. Canta, N. Oggioni, A. Malacrida, M. Corbo, G. Cavaletti, M. Peviani, D. Curti, G. Dondio, S. Collina. Toward the identification of neuroprotective agents: g-scale synthesis, pharmacokinetic evaluation and CNS distribution of (R)-RC-33, a promising Sigma1 receptor agonist, Future Medicinal Chemistry 8 (2016) 287-295.

[9] S.Y. Tsai, T. Hayashi, B.K. Harvey, Y. Wang, W.W. Wu, R.F. Shen, Y. Zhang, K.G. Becker, B.J. Hoffer, T.P. Su. Sigma-1 receptors regulate hippocampal dendritic spine formation via a free radical-sensitive mechanism involving Rac1xGTP pathway, Proc. Natl. Acad. Sci. U.S.A. 106 (2009) 22468-22473.

[10] B. Wang, R. Rouzier, C.T. Albarracin, A. Sahin, P. Wagner, Y. Yang, T.L. Smith, F. Meric Bernstam, A.C. Marcelo, G.N. Hortobagyi, L. Pusztai. Expression of sigma 1 receptor in human breast cancer, Breast Cancer Research Treatment 87 (2004) 205-214.

[11] T. Maurice, T.P. Su. The pharmacology of sigma-1 receptors, Pharmacol. Ther., 124 (2009) 195-206.

[12] M. Peviani, E. Salvaneschi, L. Bontempi, A. Petese, A. Manzo, D. Rossi, M. Salmona, S. Collina, P. Bigini, D. Curti. Neuroprotective effects of the Sigma-1 receptor (S1R) agonist PRE-084, in a mouse model of motor neuron disease not linked to SOD1 mutation, Neurobiol. Dis. 62 (2014) 218-232.

[13] B.A. Spruce, L.A. Campbell, N. McTavish, M.A. Cooper, M.V. Appleyard, M. O'Neill, J. Howie, J. Samson, S. Watt, K. Murray, D. McLean, N.R. Leslie, S.T. Safrany, M.J. Ferguson, J.A. Peters, A.R. Prescott, G. Box, A. Hayes, B. Nutley, F. Raynaud, C.P. Downes, J.J. Lambert, A.M. Thompson, S. Eccles. Small molecule antagonists of the sigma-1 receptor cause selective release of the death program in tumor and self-reliant cells and inhibit tumor growth in vitro and in vivo, Cancer Research 64 (2004) 4875-4886.

[14] E. Aydar, P. Onganer, R. Perrett, M.B. Djamgoz, C.P. Palmer. The expression and functional characterization of sigma (sigma) 1 receptors in breast cancer cell lines, Cancer Letters 242 (2006) 245-257.

[15] D. Crottes, H. Guizouarn, P. Martin, F. Borgese, O. Soriani. The sigma-1 receptor: a regulator of cancer cell electrical plasticity?, Front. Physiology 4 (2013) 175.

[16] M. Happy, J. Dejoie, C.K. Zajac, B. Cortez, K. Chakraborty, J. Aderemi, M. Sauane. Sigma 1 Receptor antagonist potentiates the anti-cancer effect of p53 by regulating ER stress, ROS production, Bax levels, and caspase-3 activation, Biochemical and Biophysical Research Communications. 456 (2015) 683-688.

[17] C. Zeng, S. Vangveravong, J. Xu, K.C. Chang, J. Xu, R.S. Hotchkiss, L. Jones, K.T. Wheeler, D. Shen, Z.P. Zhuang, H.F. Kung, R.H. Mach. Subcellular localization of sigma-2 receptors in breast cancer cells using two-photon and confocal microscopy, Cancer Res. 67 (2007) 6708-6716.

[18] G. Cassano, G. Gasparre, M. Niso, M. Contino, V. Scalera, N.A. Colabufo. F281, synthetic agonist of the sigma-2 receptor, induces Ca2+ efflux from the endoplasmic reticulum and mitochondria in SK-N-SH cells, Cell Calcium 45 (2009) 340–345.

[19] J. Xu, C. Zeng, W. Chu, F. Pan, J.M. Rothfuss, F. Zhang, Z. Tu, D. Zhou, D. Zeng, S. Vangveravong, F. Johnston, D. Spitzer, K.C. Chang, R.S. Hotchkiss, W.G. Hawkins,

K.T. Wheeler, R.H. Mach. Identification of the PGRMC1 protein complex as the putative sigma-2 receptor binding site, Nature Comm. 2 (2011) 380.

[20] S.B. Hellewell, W.D. Bowen. A sigma-like binding site in rat pheochromocytoma (PC12) cells: decreased affinity for (+)-benzomorphans and lower molecular weight suggest a different sigma receptor form from that of guinea pig brain, Brain Res. 527 (1990) 244-253.

[21] I.S. Ahmed, H.J. Rohe, K.E. Twist, M.N. Mattingly, R.J. Craven. Progesterone receptor membrane component 1 (Pgrmc1): a heme-1 domain protein that promotes tumorigenesis and is inhibited by a small molecule, J. Pharmacol. Exp. Ther. 333 (2010) 564-573.

[22] R.H. Mach, C.R. Smith, I. Al-Nabulsi, B.R. Whirrett, S.R. Childers, K.T. Wheeler. Sigma 2 receptors as potential biomarkers of proliferation in breast cancer, Cancer Res. 57 (1997) 156-161.

[23] K.T. Wheeler, L.M. Wang, C.A. Wallen, S.R. Childers, J.M. Cline, P.C. Keng, R.H. Mach. Sigma-2 receptors as a biomarker of proliferation in solid tumours, Br. J. Cancer 82 (2000) 1223-1232.

[24] N.A. Colabufo, F. Berardi, M. Contino, S. Ferorelli, M. Niso, R. Perrone, A. Pagliarulo, P. Sapanuro, V. Pagliarulo. Correlation between sigma2 receptor protein expression and histopathologic grade in human bladder cancer, Cancer Lett. 237 (2006) 83-88.

[25] H. Kashivagi, J.E. McDunn, P.O. Simon, P.S. Goedegebure, J. Xu, L. Jones, K. Chang, F. Johnston, K. Trinkaus, R.S. Hotchkiss, R.H. Mach, W.G. Hawkins. Selective sigma-2 ligands preferentially bind to pancreatic adenocarcinomas: applications in diagnostic imaging and therapy, Mol. Cancer 6 (2007) 48.

[26] C. Zeng, J. Rothfuss, J. Zhang, W. Chu, S. Vangveravong, Z. Tu, F. Pan, K.C. Chang, R. Hotchkiss, R.H. Mach. Sigma-2 ligands induce tumour cell death by multiple signalling pathways, British Journal of Cancer 106 (2012) 693–701.

[27] S.M. Husbands, S. Izenwasser, T. Kopajtic, W.D. Bowen, B.J. Vilner, J.L. Katz, A.H. Newman. Structure-Activity Relationships at the Monoamine transporters and σ receptors for a novel series of 9-[3-(*cis*-3,5-dimethyl-1-piperazinyl)-propyl]carbazole (Rimcazole) analogues, J. Med. Chem. 42 (1999) 4446-4455.

[28] Y.S. Huang, H.L. Lu, L.J. Zhang, Z. Wu. Sigma-2 Receptor Ligands and Their Perspectives in Cancer Diagnosis and Therapy, Medicinal Research Reviews 34 (2014) 532–566.

[29] (a) S. Collina, G. Loddo, M. Urbano, L. Linati, A. Callegari, F. Ortuso, S. Alcaro, C. Laggner, T. Langer, O. Prezzavento, G. Ronsisvalle, O. Azzolina. Design, synthesis, and SAR analysis of novel selective sigma1 ligands, Bioorg. Med. Chem. 15 (2007) 771-783; (b) D. Rossi, M. Urbano, A. Pedrali, M. Serra, D. Zampieri, M.G. Mamolo, C. Laggner, C. Zanette, C. Florio, D. Shepmann, B. Wünsch, O. Azzolina, S. Collina. Design, synthesis and SAR analysis of novel selective sigma1 ligands (Part 2), Bioorg. Med. Chem. 18 (2010) 1204-1212; (c) D. Rossi, A. Pedrali, M. Urbano, R. Gaggeri, M. Serra, L. Fernandez, M. Fernandez, J. Caballero, S. Rosinsvalle, O. Prezzavento, D. Shepmann, B. Wünsch, M. Peviani, D. Curti, O. Azzolina, S. Collina. Identification of a potent and selective σ1 receptor agonist potentiating NGF-induced neurite outgrowth in PC12 cells, Bioorg. Med. Chem. 19 (2011) 6210-6224; (d) D. Rossi, A. Marra, P. Picconi, M. Serra, L. Catenacci, M. Sorrenti, E. Laurini, M. Fermeglia, S. Pricl, S. Brambilla, N. Almirante, M. Peviani, D. Curti, S. Collina. Identification of RC-33 as a potent and selective σ1 receptor agonist potentiating NGF-induced neurite outgrowth in PC12 cells. Part 2: g-scale synthesis, physicochemical characterization and in vitro metabolic stability, Bioorg. Med. Chem. 21 (2013) 2577-2586.

[30] V. Pace, F. Martínez, M. Fernández, J.V. Sinisterra, A.R. Alcántara. Highly Efficient Synthesis of New α-Arylamino-α′-chloropropan-2-ones *via* Oxidative Hydrolysis of Vinyl Chlorides Promoted by Calcium Hypochlorite, Advanced Synthesis & Catalysis. 351 (2009) 3199-3206.

[31] (a) D. Rossi, A. Pedrali, R. Gaggeri, A. Marra, L. Pignataro, E. Laurini, V. DalCol, M. Fermeglia, S. Pricl, D. Schepmann, B. Wünsch, M. Peviani, D. Curti, S. Collina. Chemical, pharmacological, and in vitro metabolic stability studies on enantiomerically pure RC-33 compounds: promising neuroprotective agents acting as σ1 receptor agonists, Chem. Med. Chem. 8 (2013) 1514-1527; (b) D. Rossi, A. Pedrali, A. Marra, L. Pignataro, D. Schepmann, B. Wünsch, L. Ye, K. Leuner, M. Peviani, D. Curti, O. Azzolina, S. Collina. Studies on the enantiomers of RC-33 as neuroprotective agents: isolation, configurational assignment, and preliminary biological profile, Chirality, 25 (2013) 814-

822; (c) R. Gaggeri, D. Rossi, S. Collina, B. Mannucci, M. Baierl, M. Juza. Quick development of an analytical enantioselective high performance liquid chromatography separation and preparative scale-up for the flavonoid Naringenin, J Chromatogr A. 1218 (2011) 5414-22; (d) D. Rossi, A. Marra, M. Rui, S. Brambilla, M. Juza, S. Collina. "Fit-for-purpose" development of analytical and (semi)preparative enantioselective high performance liquid and supercritical fluid chromatography for the access to a novel σ1 receptor agonist, J. Pharm. Biomed. Anal. 118 (2016) 363-9; (e) D. Rossi, V. Talman, G. Boije Af Gennäs, A. Marra, P. Picconi, R. Nasti, M. Serra, J. Ann, M. Amadio, A. Pascale, R.K. Tuominen, J. Yli-Kauhaluoma, J. Lee, S. Collina. Beyond the affinity for protein kinase C: exploring 2-phenyl-3-hydroxypropyl pivalate analogues as C1 domain-targeting ligands, Med. Chem. Comm. 6 (2015) 547-554.

[32] D. Rossi, A. Marra, M. Rui, E. Laurini, M. Fermeglia, S. Pricl, D. Schepmann, B. Wünsch, M. Peviani, D. Curti, S. Collina. A step forward in the sigma enigma: a role for chirality in the sigma1 receptor–ligand interaction?, MedChemComm. 6 (2015) 138-146.

[33] E. Laurini, V. Dal Col, M.G. Mamolo, D. Zampieri, P. Posocco, M. Fermeglia, V. Vio, S. Pricl. Homology Model and Docking-Based Virtual Screening for Ligands of the σ1 Receptor, ACS Med. Chem. Lett. 2 (2011) 834-839.

[34] E. Laurini, D. Marson, V. Dal Col, M. Fermeglia, M.G. Mamolo, D. Zampieri, L. Vio, S. Pricl. Another brick in the wall. Validation of the σ1 receptor 3D model by computer-assisted design, synthesis, and activity of new σ1 ligands, Mol. Pharmaceutics 9 (2012) 3107-3126.

[35] S. Brune, D. Schepmann, K.H. Klempnauer, D. Marson, V. Dal Col, E. Laurini, M. Fermeglia, B. Wünsch, S. Pricl. The sigma enigma: in vitro/in silico site-directed mutagenesis studies unveil σ1 receptor ligand binding, Biochem. 53 (2014) 2993 - 3003.

[36] I. Massova, P.A. Kollman. Combined molecular mechanical and continuum solvent approach (MM-PBSA/GBSA) to predict ligand binding, Perspectives in Drug Discovery and Design. 18 (2000) 113-135.

[37] Y. Zhang, Y. Huang, P. Zhang, X. Gao, R.B. Gibbs, S. Li. Incorporation of a selective sigma-2 receptor ligand enhances uptake of liposomes by multiple cancer cells, Int. J. Nanomedicine. 7 (2012) 4473-85.

[38] V. Mégalizzi, V. Mathieu, T. Mijatovic, P. Gailly, O. Debeir, N. De Neve, M. Van Damme, G. Bontempi, B. Haibe-Kains, C. Decaestecker, Y. Kondo, R. Kiss, F. Lefranc. 4-IBP, a sigma1 receptor agonist, decreases the migration of human cancer cells, including glioblastoma cells, in vitro and sensitizes them in vitro and in vivo to cytotoxic insults of proapoptotic and proautophagic drugs, Neoplasia. 9 (2007) 358-69.

[39] D. Das, L. Persaud, J. Dejoie, M. Happy, O. Brannigan, D. De Jesus, M. Sauane. Tumor necrosis factor-related apoptosis-inducing ligand (TRAIL) activates caspases in human prostate cancer cells through sigma 1 receptor, Biochem Biophys Res Commun. 2016 Jan 11. pii: S0006-291X(16)30055-9.

[40] C.S. John, B.J. Vilner, B.C. Geyer, T. Moody, W.D. Bowen. Targeting sigma receptor-binding benzamides as in vivo diagnostic and therapeutic agents for human prostate tumors, Cancer Res. 59 (1999) 4578-83.

[41] S. Okuyama, A. Nakazato. NE-100: A novel sigma receptor antagonist, CNS Drug Rev. 2 (1999) 226–237.

[42] C. Zeng, J.M. Rothfuss, J. Zhang, S. Vangveravong, W. Chu, S. Li, Z. Tu, J. Xu, R.H. Mach. Functional assays to define agonists and antagonists of the sigma-2 receptor, Analytical Biochemistry. 448 (2014) 68-74.

[43] M. Takebayashi, T. Hayashi, T.P. Su. Nerve growth factor-induced neurite sprouting in PC12 cells involves sigma-1 receptors: implications for antidepressants, J. Pharmacol. Exp. Ther. 303 (2002) 1227-1237.

[44] T. Nishimura, T. Ishima, M. Iyo, K. Hashimoto. Potentiation of nerve growth factor-induced neurite outgrowth by fluvoxamine: role of sigma-1 receptors, IP3 receptors and cellular signaling pathways, PLoS One 3 (2008) e2558.

[45] T. Ishima, K. Hashimoto. Potentiation of nerve growth factor-induced neurite outgrowth in PC12 cells by ifenprodil: the role of sigma-1 and IP3 receptors, PLoS One 7 (2012) e37989.

[46] M.J. Robson, B. Noorbakhsh, M.J. Seminerio, R.R. Matsumoto. Sigma-1 receptors: potential targets for the treatment of substance abuse, Curr. Pharm. Des. 18 (2012) 902-19.

[47] T. Ishima, Y. Fujita, K. Hashimoto. Interaction of new antidepressants with sigma-1 receptor chaperones and their potentiation of neurite outgrowth in PC12 cells, Eur. J. Pharmacol. 727 (2014) 167-73.

[48] I.S. Ahmed, C. Chamberlain, R.J. Craven. S2R (Pgrmc1): the cytochromerelated sigma-2 receptor that regulates lipid and drug metabolism and hormone signaling, Expert Opin. Drug Metab. Toxicol. 8 (2012) 361–370.

[49] S.U. Mir, I.S. Ahmed, S. Arnold, R.J. Craven. Elevated progesterone receptor membrane component 1/sigma-2 receptor levels in lung tumors and plasma from lung cancer patients, Int. J. Cancer. 131 (2012) E1–9.

[50] S.U. Mir, S.R. Schwarze, L. Jin, J. Zhang, W. Friend, S.S. Miriyala, D. Clair, R.J. Craven. Progesterone receptor membrane component 1/Sigma-2 receptor associates with MAP1LC3B and promotes autophagy, Autophagy 9 (2013) 1566–1578.

[51] C. Abate, M. Niso, V. Infantino, A. Menga, F. Berardi. Elements in support of the 'non-identity' of the PGRMC1 protein with the σ2 receptor, Eur J Pharmacol. 5 (2015) 16-23.

[52] U.B. Chu, T.A. Mavlyutov, M.L. Chu, H. Yang, A. Schulman, C. Mesangeau, C.R. McCurdy, L.W. Guo, A.E. Ruoho. The Sigma-2 Receptor and Progesterone Receptor Membrane Component 1 are Different, E. Bio. Medicine. 11 (2015) 1806-13.

[53] A.E. Ruoho, L.W. Guo, A.R. Hajipour, K. Karaoglu, T.A. Mavlyutov, T. A.; U.B. Chu, J. Yang. Will the true sigma-2 receptor please stand up?, San Diego, 2013. Neuroscience Meeting.

[54] A. van Waarde, A.A. Rybczynska, N.K. Ramakrishnan, K. Ishiwata, P.H. Elsinga, R.A. Dierckx. Potential applications for sigma receptor ligands in cancer diagnosis and therapy, Biochim. Biophys. Acta 1848 (2014) 2703-2714.

[55] C. Lee, L. Raffaghello, S. Brandhorst, F.M. Safdie, G. Bianchi, A. Martin-Montalvo, V. Pistoia, M. Wei, S. Hwang, A. Merlino, L. Emionite, R. de Cabo, V.D. Longo. Fasting cycles retard growth of tumors and sensitize a range of cancer cell types to chemotherapy, Sci Transl Med. 4 (2012) 124-27.

[56] L. Raffaghello, C. Lee, F.M. Safdie, M. Wei, F. Madia, G. Bianchi, V.D. Longo. Starvation-dependent differential stress resistance protects normal but not cancer cells against high-dose chemotherapy, Proc Natl Acad Sci U S A. 105 (2008) 8215-20.

[57] F. Safdie, S. Brandhorst, M. Wei, W. Wang, C. Lee, S. Hwang, P.S. Conti, T.C. Chen, V.D. Longo. Fasting enhances the response of glioma to chemo- and radiotherapy, PLoS One 7 (2012) e44603.

[58] I. Caffa, V. D'Agostino, P. Damonte, D. Soncini, M. Cea, F. Monacelli, P. Odetti, A. Ballestrero, A. Provenzani, V.D. Longo, A. Nencioni. Fasting potentiates the anticancer activity of tyrosine kinase inhibitors by strengthening MAPK signaling inhibition, Oncotarget 6 (2015) 11820-32.

[59] S. de Groot, M.P. Vreeswijk, M.J. Welters, G. Gravesteijn, J.J. Boei, A. Jochems, D. Houtsma, H. Putter, J.J. van der Hoeven, J.W. Nortier, H. Pijl, J.R. Kroep. The effects of short-term fasting on tolerance to (neo) adjuvant chemotherapy in HER2-negative breast cancer patients: a randomized pilot study, BMC Cancer 15 (2015) 652.

[60] J. Menis, B. Hasan, B. Besse. New clinical research strategies in thoracic oncology: clinical trial design, adaptive, basket and umbrella trials, new end-points and new evaluations of response, Eur. Respir. Rev. 23 (2014) 367-78.

[61] A.S. Bura, T. Guegan, D. Zamanillo, J.M. Vela, R. Maldonado. Operant self-administration of a sigma ligand improves nociceptive and emotional manifestations of neuropathic pain, Eur J Pain. 17 (2013) 832-43.

[62] L. Romero, D. Zamanillo, X. Nadal, R. Sanchez-Arroyos, I. Rivera-Arconada, A. Dordal, A. Montero, A. Muro, A. Bura, C. Segalés, M. Laloya, E. Hernández, E. Portillo-Salido, M. Escriche, X. Codony, G. Encina, J. Burgueño, M. Merlos, J.M. Baeyens, J. Giraldo, J.A. López-García, R. Maldonado, C.R. Plata-Salamán, J.M. Vela. Pharmacological properties of S1RA, a new sigma-1 receptor antagonist that inhibits neuropathic pain and activity-induced spinal sensitization, Br J Pharmacol. 166 (2012) 2289-306.

[63] J.L. Diaz, D. Zamanillo, J. Corbera, J.M. Baeyens, R. Maldonado, M.A. Pericas, J.M. Vela, A. Torrens. Selective sigma-1 (sigma1) receptor antagonists: Emerging target for the treatment of neuropathic pain, Cent Nerv Syst Agents Med Chem. 9 (2009) 172-83.

[64] F. Weber, S. Brune, K. Korpis, P.J. Bednarski, E. Laurini, V. Dal Col, S. Pricl, D. Schepmann, B. Wünsch. Synthesis, pharmacological evaluation, and σ1 receptor

interaction analysis of hydroxyethyl substituted piperazines, J. Med. Chem. 57 (2014) 2884-2894.

[65] D.A. Case, J.T. Berryman, R.M. Betz, D.S. Cerutti, T.E. Cheatham, III, T.A. Darden, R.E. Duke, T.J. Giese, H. Gohlke, A.W. Goetz, N. Homeyer, S. Izadi, P. Janowski, J. Kaus, A. Kovalenko, T.S. Lee, S. LeGrand, P. Li, T. Luchko, R. Luo, B. Madej, K.M. Merz, G. Monard, P. Needham, H. Nguyen, H.T. Nguyen, I. Omelyan, A. Onufriev, D.R. Roe, A. Roitberg, R. Salomon-Ferrer, C.L. Simmerling, W. Smith, J. Swails, R.C. Walker, J. Wang, R.M. Wolf, X. Wu, D.M. York and P.A. Kollman (2015), AMBER 2015, University of California, San Francisco.

[66] W.L. Jorgensen, J. Chandrasekhar, J.D. Madura, R.W. Impey, M.L. Klein. Comparison of simple potential functions for simulating liquid water, J. Chem. Phys. 79 (1983) 926-935.

[67] V. Tsui, D.A. Case. Theory and applications of the generalized Born solvation model in macromolecular simulations, Biopolymers 56 (2000) 275-291.

[68] A. Onufriev, D. Bashford, D.A. Case. Modification of the generalized Born model suitable for macromolecules. J. Phys. Chem. B 104 (2000) 3712-3720.

Highlights

- Design, synthesis and binding affinity evaluation of racemic and entiomeric pan-Sigma Receptor (SR) modulators.
- S1R agonist/antagonist profile
- Cytotoxic activity toward a panel of cancer cell lines.
- Compound **3** (RC-106) highlighted a promising cytotoxic activity on a panel of cancer cell lines of different tumors, representative of various cancer expressing both SRs.